REAL-TIME DATA QUALITY MONITORING SYSTEM FOR THE CMS MUON GEM DETECTOR AT THE LHC

An Undergraduate Research Scholars Thesis

by

ROBERT KING

Submitted to the Undergraduate Research Scholars program
Texas A&M University
in partial fulfillment of the requirements for the degree of

UNDERGRADUATE RESEARCH SCHOLAR

Approved by Research Advisor: Dr. Alexei Safonov

May 2017

Major: Physics, Electrical Engineering

ABSTRACT

Real-Time Data Quality Monitoring System for the CMS Muon GEM Detector at the LHC

Robert King
Department of Physics, Electrical Engineering
Texas A&M University

Research Advisor: Dr. Alexei Safonov
Department of Physics and Astonomy
Texas A&M University

The new operational conditions associated with the high luminosity upgrade of the Large Hadron Collider (LHC) at CERN requires an upgrade of the muon system in the forward region of the Compact Muon Solenoid (CMS) detector. The upgrade will allow the detector to record and handle a higher rate of particles. A major element of this upgrade is the implementation of new gas electron multiplier (GEM) detectors in the pseudorapidity region $1.6 < \eta < 2.4$, where the background particle rates are highest [1]. These detectors will add redundancy to the existing muon system in this region, and improve performance by allowing more intelligent triggering algorithms to reduce the trigger rate. The data acquisition electronics on these detectors must be thoroughly tested to verify that the data produced by the detector is valid, and that there are no hardware or firmware problems before the GEMs are installed underground in CMS. Once installed, the system must also be monitored to verify that no problems arise during normal data-taking operations. I discuss the software being developed to read out and process the data produced by the detectors, and the methods used to identify hardware and firmware problems using this

information in real time.

ACKNOWLEDGMENTS

First and foremost I would like to acknowledge Misha Dalchenko, the coauthor of the light DQM software which is the primary work of my thesis. None of my contribution would be possible without your help. Thank you for teaching me how to code like a physicist, find my own bugs, and use Google effectively. Next I would like to thank Jason Gilmore, Evaldas Juska, Jared Sturdy, Brian Dorney, and the rest of the GEM collaboration for their guidance and help with my work. Finally, I must thank Alexei Safonov for providing me with endless opportunities to succeed. Thank you for all the doors that you have opened up for me.

TABLE OF CONTENTS

Page

LIST OF FIGURES

FIGURE Page

LIST OF TABLES

TABLE Page

CHAPTER 1

INTRODUCTION

The Large Hadron Collider (LHC) is the world's largest particle collider, consisting of a 27-kilometer ring approximately 100 meters underground [2]. Accelerated particles (protons or lead ions) travel anti-parallel in bunches and are made to collide at four different collision zones around the ring. Each collision point is associated with a different experimental detector, and has unique design and physics goals.

The Compact Muon Solenoid (CMS) is one of these detectors, and is the experiment where my research has been conducted. CMS is a general-purpose detector, designed to be used in physics ranging from B-physics and high precision tests of the Standard Model to searches for supersymmetry, extra dimensions, and other physics outside of the Standard Model. One of the key components of CMS is its muon system. This system identifies muons among other particles produced in LHC collisions. It furthermore tracks the path of these muons through the detector in order to determine their momentum and provide information to the global muon trigger. The muon trigger filters the data stream to focus on interesting events in terms of physics analysis.

The current luminosity results in approximately 10^9 inelastic events per second [3]. This rate causes the detector electronics to produce more data than can be handled by physical hardware capabilities, and must be filtered using a specially-developed trigger system. The data from the muon detectors is one of the most important components in event reconstruction for both triggering and understanding interesting physical events beyond the Standard Model.

One of the primary goals of the Large Hadron Collider and accompanying experiments

is to search for new physics outside of the Standard Model, in order to explain concepts such as the origin of mass, dark matter, and dark energy [2]. Much of this new physics is theorized to have a rather small production cross-section. In order to see such interesting events, the probability of having such collisions within a reasonable amount of time is increased by raising the luminosity of the beam. To handle higher luminosity, CMS and other experiments must upgrade their detectors and electronics to handle the corresponding higher flux of particles passing through the detectors.

One major upgrade that CMS has proposed to handle the increase in beam luminosity is the addition of Triple-Gas Electron Multiplier (GEM) detectors in the first muon station [1]. These detectors are set to be placed in pseudorapidity region $1.6 < \eta < 2.4$, where particle flux density is large. The additional detector chambers will improve the muon trigger at a critical position by increasing the path length traversed by muons through the first detection layer of the CMS muon system. This increased path length allows for a better momentum resolution and for a more precise local trigger. It will also reduce the large contribution to the overall muon trigger rate from the backgrounds in the high-eta region of the system.

In order to have a viable muon system, all chambers must have high-quality and high-speed data acquisition (DAQ) electronics. The GEM DAQ electronics are in charge of transmitting the muon tracking data to off-detector boards which then connect to the CMS central DAQ system, as well as transmitting trigger data to the CMS CSC trigger system. A separate data quality monitoring (DQM) system is also being implemented to validate the data being readout from the GEM electronics and debug hardware problems that arise during development, production, and normal data-taking.

This thesis will outline the development of the methods to control the GEM data acquisition electronics and data quality monitoring system. Chapter II will take an in-depth look at where GEM detectors fit into CMS and the muon system, and the current proposed

method of integrating GEM data into the muon trigger. Chapter III will detail the current GEM electronic system in full. Chapter IV will include the data quality monitoring and online control software that was created for the electronics. Chapter V will discuss the performance of the GEMs, including simulation, data taken, and errors encountered with the system. Final prospects including current on-going developments and future improvements are also discussed. Finally, we conclude with Chapter VI.

CHAPTER 2

MUON DETECTORS AT THE CMS EXPERIMENT

Muons play a key role in the physics program at the LHC. Many interesting physics processes are predicted to have a sizable cross-section which include muons in the final state. This includes, but is not limited to, a Standard Model Higgs boson decaying into two Z bosons which in turn produce 4 leptons [4], where the leptons are either electrons or muons. Muons are an excellent detection candidate because of their ability to penetrate through matter without radiative losses, among other reasons. Muons also appear in the search for new resonances beyond the Standard Model. This chapter will explore how muons are detected within CMS, and introduce the need for the GEM upgrade to the muon system.

2.1 The Large Hadron Collider

The Large Hadron Collider (LHC) at CERN is the most powerful particle accelerator in the world. It consists of a 27-kilometer underground ring containing superconducting magnets which guide two beams of particles travelling antiparallel around at speeds close to the speed of light. These particles travel in bunches and are made to collide at four different collision points. Every collision point is associated with a different experiment to detect events for a wide range of particle physics research. There are six different experiments located at the LHC complex, four of which are larger, primary detectors. Each of these four primary detectors are located at one collision point around the LHC ring, shown in Fig. 2.1.

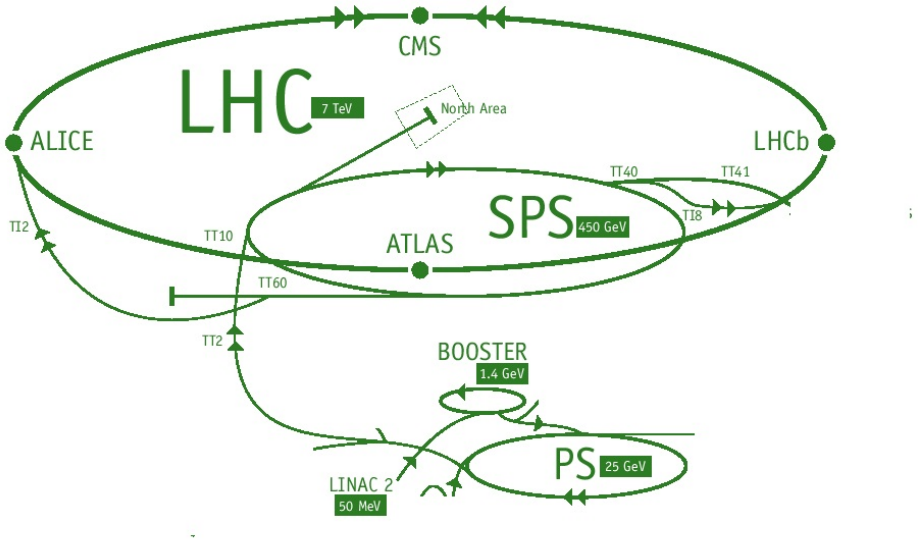

Figure 2.1: Large Hadron Collider Rings

2.2 Compact Muon Solenoid

Compact Muon Solenoid (CMS) is located on the north side of the LHC ring and consists of a 13-m long, 6-m-inner-diameter magnetic core surrounded by muon detectors [3]. The bore of the magnetic core contains the inner tracker and calorimetry, split into separate hadron and electromagnetic calorimeters. A superconducting solenoid produces a uniform 4-T magnetic field inside the barrel of CMS. There are additionally two endcaps on CMS, containing a very-forward calorimeter as well as additional muon detectors. All of these systems can be seen in the perspective view shown in Fig. 2.2.

2.3 Muon System

Surrounding the magnetic core of the CMS detector is the muon system. It consists of about 25,000 m^2 of detection area in total. The muon system is broken into two parts: the

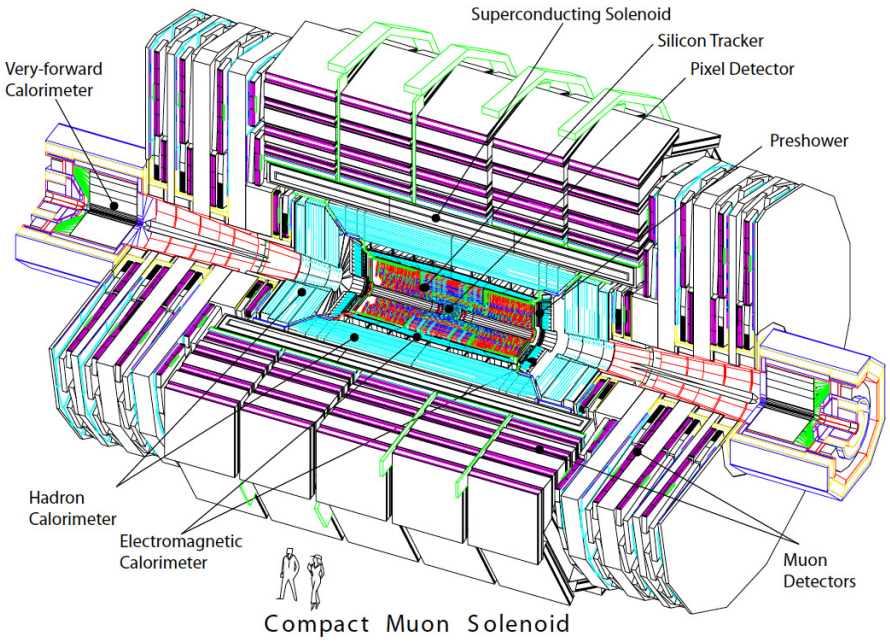

Figure 2.2: A Perspective View of the CMS Detector

barrel region, surrounding the magnetic core, and the two endcaps. Because the endcaps are closer to the beamline, in the high-eta range of the detector, the particle rate is much higher than in the barrel region. The muon system is located beyond several layers of trackers, calorimetry, and iron (magnetic return yoke), which absorb almost all particles other than muons and neutrinos. This allows confidence than most hits in the muon system are muons, because neutrinos will have no noticeable interaction with the detectors.

2.3.1 Purpose

The muon system has three primary functions: muon identification, momentum measurement, and triggering. [3] Due to the thick iron flux-return yoke of the magnet and hadron absorption of the rest of the inner systems, muon identification efficiency is around 95-99% except for small transition regions between systems. The amount of punchthrough, or non-muon particles, which reach the muon system, is small in the first muon station and

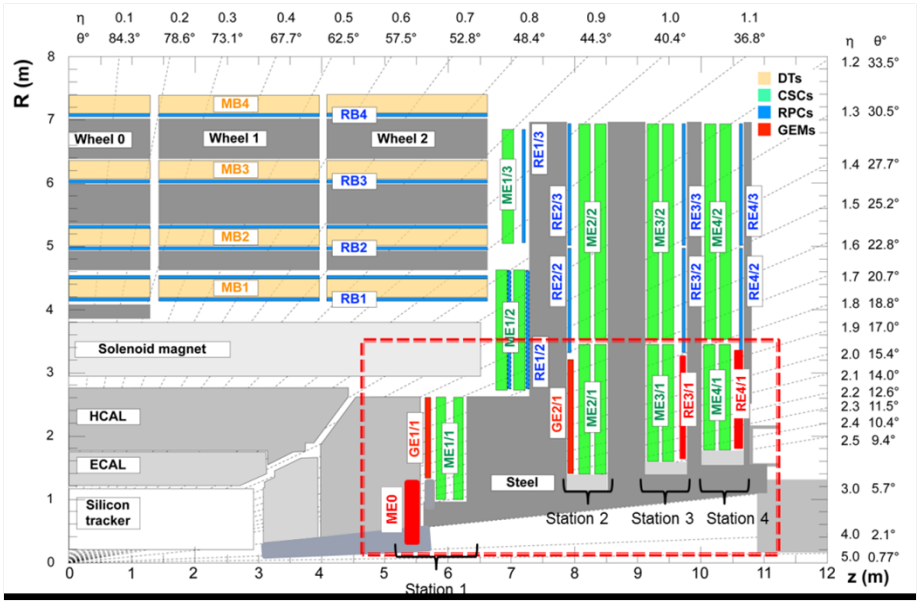

Figure 2.3: Cross-section of the CMS detector, with proposed upgrade chambers in red

effectively negligible in other stations. In other words, hits recorded in the muon system are always considered to be muon candidates, because the vast majority of other particles are absorbed before they reach the muon system.

Muons bend as they travel through the magnetic field in the solenoid due to the Lorentz force:

$$\mathbf{F} = \frac{q}{m}\mathbf{p} \times \mathbf{B} \tag{2.1}$$

Each time a muon passes through a layer of the muon system producing hits in the detector, the hit is recorded as a point in space. As the muon traverses the entire muon system, a track is formed from these points. The muon's trajectory can later be reconstructed using the recorded track. The knowledge that the particle is a muon, thus having a known charge-to-mass ratio, and the curvature of the reconstructed trajectory allows the calculation of the muon's momentum.

It is not feasible for the muon system electronics to record and capture every hit from the millions of events per second produced in CMS. A large rate reduction procedure is set in place in the electronics, which is known as the muon trigger. The trigger involves multiple steps to make a decision on which events are considered "interesting" and worth saving to analyze offline. The vast majority of events in CMS are not interesting because they result from elastic or semi-elastic scattering rather than inelastic, so dumping these events is no loss to physics results.

Because the bunch crossing (BX) rate is 40 MHz, the trigger logic must handle new data every 25 ns. With the help of a large memory buffer to pipeline the high-resolution data, this decision can take up to a maximum latency of 3.2 μs. Due to this very strict time restraint, the trigger logic breaks down the decision into steps. It uses regional components to make local trigger decisions which are passed to higher levels and ultimately result in a Global Level-1 (L1) trigger. This trigger tells all chambers to save their high-resolution data and send it offline for higher-level processing before being permanently stored.

2.3.2 Components

The muon system is composed of drift tube (DT) chambers, cathode strip chambers (CSC), and resistive plate chambers (RPC). DTs and RPCs are used in the barrel region, where the particle rate is lower and the 4-T magnetic field is uniform. The endcaps employ RPCs and CSCs, due to the greater rate-capabilities of the CSCs compared to DTs. Gas electron multiplier (GEM) detectors will soon be integrated with the current muon endcap system in the GE 1/1 upgrade during the second long shutdown (LS2) around 2019. [1] The term GE 1/1 refers to the location of the chambers: GE stands for GEM Endcap, and the numbers indicate the chambers are located at the innermost part of CMS.

2.3.3 Upgrade

Once the current LHC Phase 1 operation ends around 2022, a third long shutdown (LS3) will implement a major upgrade to the instantaneous luminosity. After the upgrade, the high luminosity LHC collider (HL-LHC) will have improved the instantaneous luminosity from 2×10^{34} cm^{-2}s^{-1} to 5×10^{34} cm^{-2}s^{-1}.

This large increase in luminosity will produce a much higher rate of collisions, and thus a higher flux of muons through the detectors. Muon trigger studies demonstrate the need for an upgrade in the endcap to maintain the trigger rates needed to meet CMS system design specifications. Major upgrades have been proposed for both a new Level-1 trigger upgrade [5] and the addition of new GEM chambers in the endcap region to solve this problem.

2.4 Gas Electron Multiplier Detectors

Gas Electron Multiplier (GEM) technology is a recently-developed strategy at gaseous particle detection. It employs thin polyimide GEM foils, containing tiny holes which amplify an applied electric field (Fig. 2.4), producing an electron-ion avalanche when a charged particle passes through and ionizes the gas within the detector. The GEM detectors under development for CMS employ three of these foils, and are thus commonly referred to as triple-GEM chambers. Three foils allows for a much larger avalanche (Fig. 2.5) and thus greater charge amplification. Figure 2.5 shows the gap sizes between the three GEM foils, with a total distance of 7 mm between drift cathode and readout PCB. The resulting large charge amplification factor (up to 10^5) allows for induced charges large enough to be read out by sensitive front-end electronics attached to the readout board.

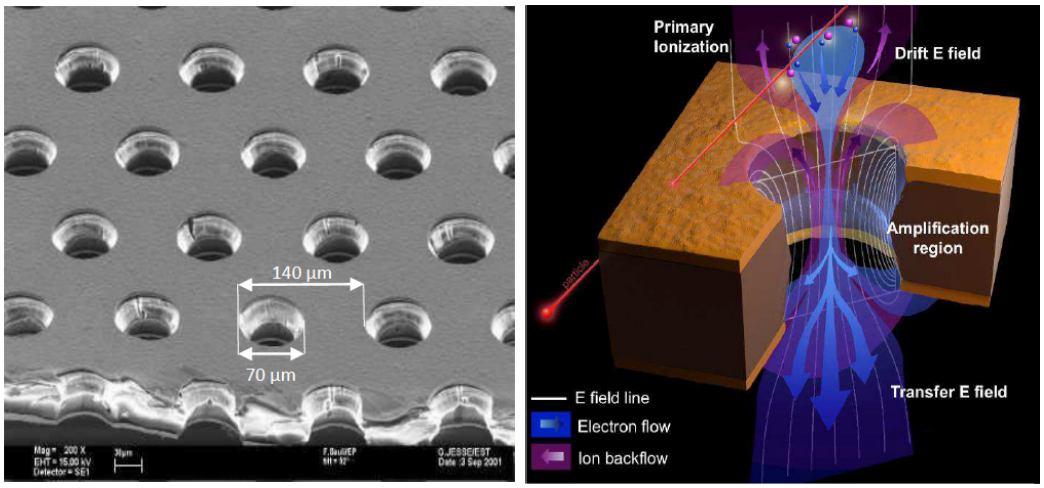

Figure 2.4: (Left) GEM foil hole dimensions; (Right) Resulting electric field lines, electron flow, and ion flow

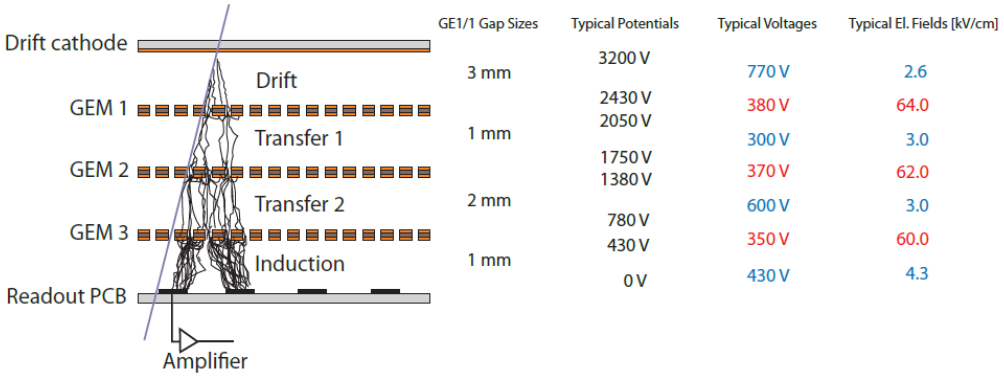

Figure 2.5: Triple-GEM chamber operation and definition of drift, transfer, and signal induction gap regions within the detector. Values for potential of 3200 V operating in Ar/CO_2 70:30 applied to the drift cathode. [1]

2.4.1 Motivation for GEMs in CMS

The location of the first proposed additional chambers was a small space between the hadron calorimeter and the already-installed CSC chambers (see GE1/1 in Fig. 2.3). Therefore, the new chambers were required to be quite thin. The design specification for

the total thickness of a single GEM chamber is only 3.5 cm [1], and are thus able to meet the thickness requirements of the upgrade. An exploded view of a single GEM chamber is shown in Figure 2.6 along with a fully-assembled super-chamber. One super-chamber contains two triple-GEM chambers attached front-to-back.

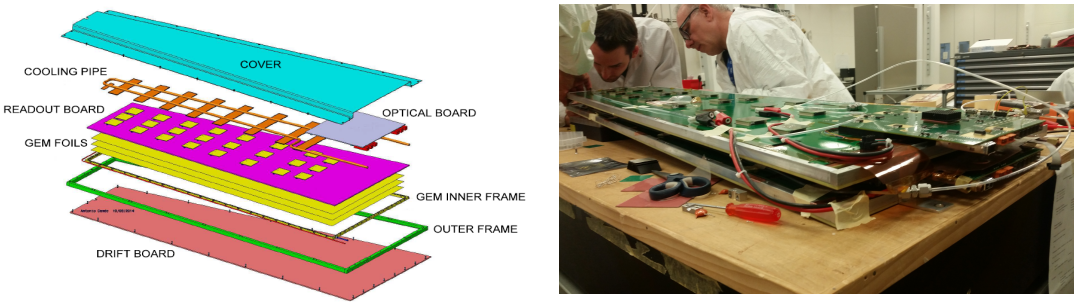

Figure 2.6: (Left) Triple-GEM chamber exploded view; (Right) fully-assembled superchamber in tracker integration facility

CHAPTER 3

REQUIREMENTS FOR THE GEM DAQ MONITORING SYSTEM

This chapter outlines the GEM DAQ hardware, which has not been developed as part of the current thesis work, but is included for completeness. The GEM detectors are responsible for providing both tracking and trigger data. Tracking data consists of high-resolution, full-granularity spatial location of muon hits associated with a single bunch-crossing. Due to its large size, this information is transmitted only on receipt of a level-1 (L1) accept trigger, also referred to as L1A. This signal is sent from the muon trigger system, and is essentially viewed as an external signal in the scope of the GEM electronics system. Trigger data is a minimized, fixed-latency "fast-OR" of multiple channels transmitted in real time to provide trigger information as quickly as possible to the muon trigger system.

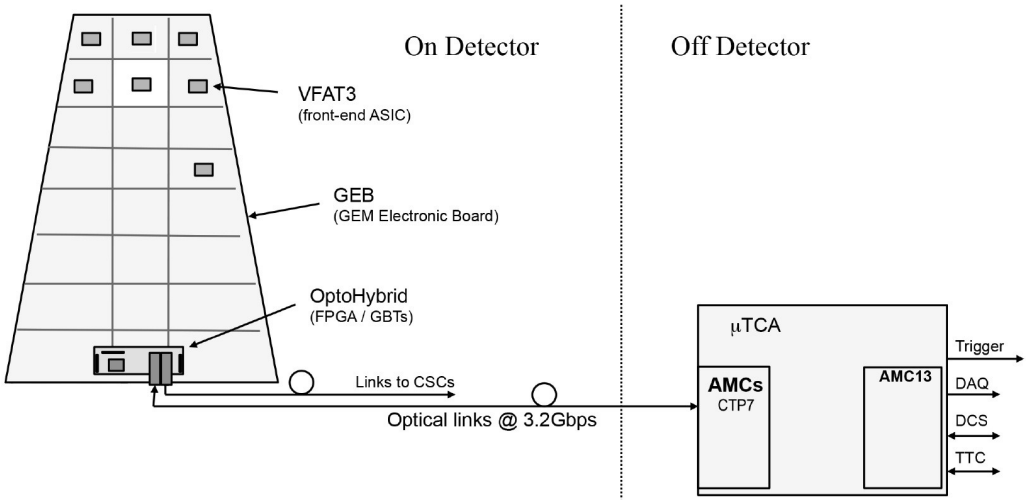

Figure 3.1: Overview of GEM data acquisition electronics system

3.1 On-Detector Electronics

The GEM detector electronics can be broken down into on-detector and off-detector electronics. The on-detector electronics are specially designed in order to operate in the high magnetic field and heavily irradiated environment within CMS. Many commercial electronics are not able to operate in such conditions, so several applications are under development at CERN. Generic developments directly related to GEM electronics include the gigabit transceiver (GBT) [6], Versatile Link [7], and DC/DC converters [8].

3.1.1 VFAT front-end ASIC

The muon detection process begins on the detector with a front-end application-specific integrated circuit (ASIC) chip, called VFAT2, adopted from the TOTEM experiment [9][10]. A new version of this chip, called VFAT3, is currently under development for specific application with triple-GEMs in CMS [11]. Each VFAT2 chip converts the charge deposited onto 128 strips of the GEM readout board to a binary value using a preamplifier, shaper, and comparator. The binary value for a channel is set if the signal on a strip is measured to be larger than a programmable threshold, so it is essentially a 1-bit comparator for every channel. The VFAT3 is expected to be used in the final GEM electronics system, and includes various improvements to the VFAT2. More information on the VFAT3 will be included in a later chapter.

3.1.2 GEM Electronics Board

Each front-end VFAT chip is connected to 128 strips on the readout board, resulting in 24 VFATs per chamber to read out every strip. The VFATs are connected to both the GEM readout board and the GEM electronics board, or GEB, as shown in Figure 3.2. The GEB is a trapezoidal printed circuit board (PCB) approximately the size of a chamber which sits on top of the chamber itself and connects to the VFATs. The purpose of the GEB is to

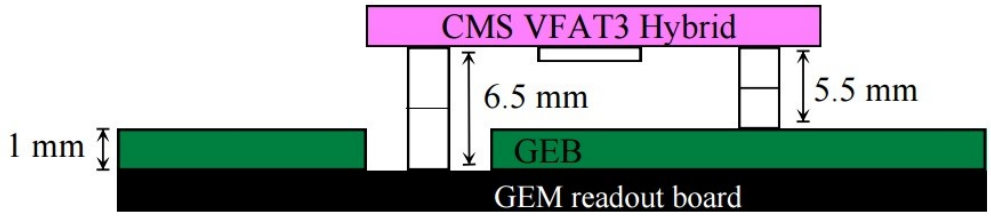

Figure 3.2: VFAT3 ASIC connection between GEM readout board and GEM electronics board

carry signals and power for the VFATs and the OptoHybrid (OH) board. Because the GEB is as large as a chamber (nearly a meter long), it is very difficult to manufacture. All of the connectors on the GEBs must be soldered by hand. Modifications are currently under development to the shape of the GEB for the third version of the board, detailed in a later chapter.

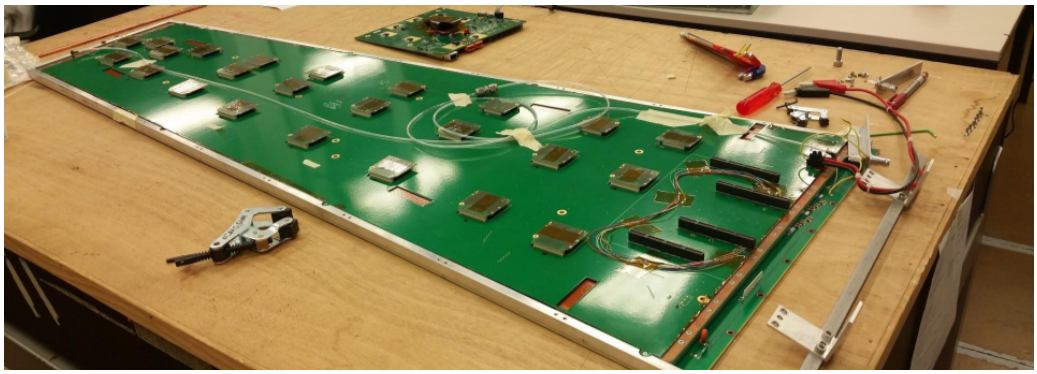

Figure 3.3: GEM chamber with fully-mounted GEBv2

3.1.3 OptoHybrid Board

The OptoHybrid (OH) board is mounted on the GEB and collects the signals from the 24 VFATs. It consists of a field-programmable gate array (FPGA), 3 gigabit transceiver

(GBT) links, and 3 small form factor pluggables (SFP) or a quad-SFP optical connector. Around 400 I/Os are necessary to connect the OH FPGA (Xilinx Virtex-6) to all 24 VFAT chips. Some of the key functions of the OH include synchronizing the VFAT data, zero-suppressing the trigger data, encoding the data into data packets, and sending them via optical links to the muon trigger and off-detector GEM electronics.

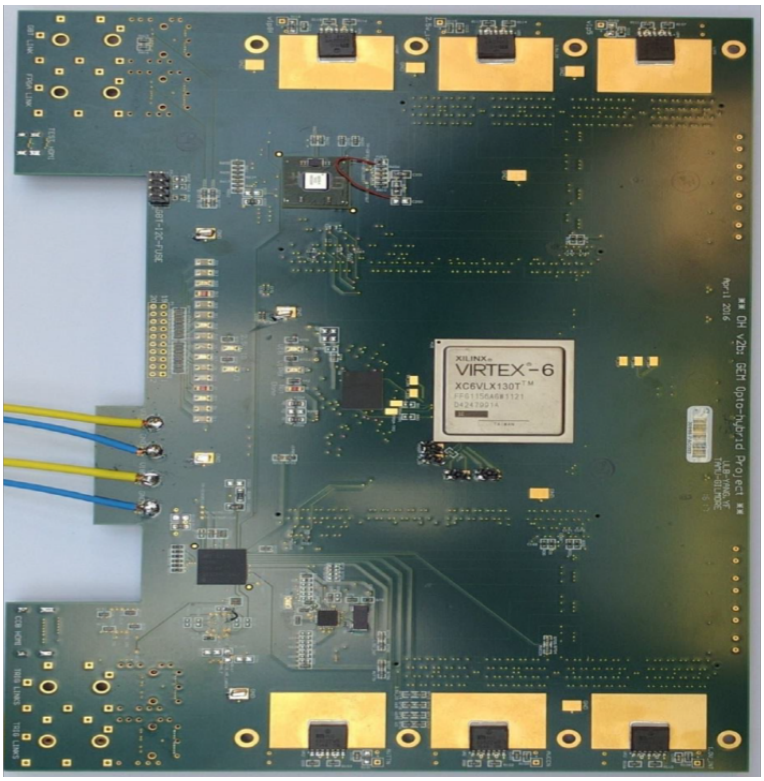

Figure 3.4: OptoHybrid version 2b

The GBT protocol is the primary design choice for communication between OH and off-detector electronics. Because this technology is still under development, a back-up solution is included until the GBT protocol has been employed and verified with the GEM electronics. The back-up solution uses an HDMI cable between the OH and a Clock and

Control Board (CCB) used by CSC chambers in CMS to enable remote recovery of the on-chamber electronics if reprogramming becomes necessary.

The GBT optical link technology provides bidirectional 4.8 Gb/s communication, depending on configuration, with the ability to recover the bunch clock, reduce input clock jitter, and distribute phase-controlled clock signals. The data bandwidth is expected to only reach 3.2 Gb/s for each fiber in the CMS GEM project. The GBT Transceiver (GBTx), located on the OH, will facilitate bidirectional communicate with VFAT3 chips and CMS central services. The CMS central services provide global timing and control signals to synchronize all electronics in CMS.

Trigger data will be sent in parallel directly to both the local CSC optical trigger motherboard (OTMB) and Muon TrackFinder (MTF) to be combined with CSC data and improve the muon trigger algorithms. Existing optical fibers currently used by the CSC electronics will be used for this communication path. These links cannot utilize the GBT protocol, however, so the 8b/10b protocol will be used instead.

3.2 Off-Detector Electronics

The GEM off-detector electronics operate under the commercial micro-TCA (μTCA) standard. μTCA aims at high data throughput (2 Tbit/s) and low probability of interruption (around 10^{-5}). It utilizes advanced mezzanine cards (AMC) which are compact, hot-swappable, and connect with a high-speed serial backplane. The preferred CMS μTCA crate, VadaTech VT892 [12], supports 12 double-width, full-height AMC cards and two μTCA Carrier Hub (MCH) slots. This crate also holds the AMC13, which connects to all other AMCs in the crate.

3.2.1 Advanced Mezzanine Card

The OH board optical fibers for each chamber connect directly to an advanced mezzanine card (AMC) in the μTCA crate. The AMC is responsible for collecting both the

tracking and trigger data packets from multiple OHs, meaning a single AMC can control several chambers simultaneously. Some coincidence-finding algorithms are performed on the trigger data and transmitted to the Muon Track Finder. The tracking data is sent to the AMC13 through the μTCA backplane to be stored offline.

There are several different AMC board architectures which could be used to fulfill the necessary role for the GEM system. Among these include GLIB, CTP7, MTF7, and MP7. The process to decide the final AMC to use in GE1/1 will be discussed in the next chapter. Only 12 AMCs can fit in a single μTCA crate.

3.2.2 AMC13 Card

The final piece of hardware in the GEM electronics chain is the AMC13, developed by Boston University [13]. The AMC13 card connects to all 12 of the AMC slots via the high-speed backplane of the μTCA crate at 5.0 Gb/s. Its main functions include distribution of clock and control signals to the entire GEM DAQ system and data acquisition from all AMCs. Communication with the AMC13 is done via IPBus over Gigabit Ethernet (GbE). Data is pushed to the CMS Front-End Driver Kit (FEDKit) interface through a 10 GB optical link. The AMC13 collects each of the event blocks from the AMCs and forms a single event block using CMS common data format. This event block is the final block sent to the DAQ online software and stored.

CHAPTER 4

DESIGN OF THE GEM DAQ MONITORING SYSTEM

The GEM data acquisition (DAQ) system has been customized at every level to meet the necessary design requirements. While the development of the detector electronics and built-in scans has not been part of the currently presented work, an overview of the full electronics and associated capabilities is included for completeness. All of the on-detector electronic boards were designed by experts within the collaboration due to the novelty of the detectors themselves. The on-detector electronics are also required to function in the large magnetic field and highly irradiated environment inside CMS, eliminating most commercial applications. Only the off-detector electronics were purchased from other sources.

One of the key boards to the performance of the system as a whole is the advanced mezzanine card (AMC), located in the μTCA crate off of the detector. This board requires high-level performance and was not designed by the GEM collaboration. As mentioned in Chapter 3, there were several boards considered to be used as the AMC for the GEM DAQ system. Of these include GLIB, CTP7, MTF7 and MP7. The GLIB (Gigabit Link Interface Board), developed by CERN, was used in the initial testing of the system. It was expected to be replaced in the final system due to the small amount of optical links on each board. One GLIB can support only 2 chambers using VFAT2s, and only one chamber using VFAT3s. This would require 72 GLIBs to support all 72 chambers in the GE1/1 upgrade. This is inconvenient and infeasible, thus, this board was never intended to be used in the final installation, but rather as a testing board to develop the initial versions of the electronics.

Table 4.1: Comparisons of different Advanced Mezzanine Cards for GEM DAQ System

AMC	Transceiver/Receivers	FPGA	RAM	Features
CTP7	67 RX @ 10 Gbs 48 TX @ 10 Gbs 13 backplane TX/RX	Virtex-7 (690T)	52 Mb	ZYNQ SoC Designer support
MP7	72 TX/RX @ 10Gbs	Up to 690T	Up to 288Mb	Configurable FPGA
MTF7	86 RX, 28 TX @ 10 Gbs	Virtex-7 (690T)	1GB	Large memory

The other boards considered were the MP7, developed by Imperial College, London, the MTF7, developed by the University of Florida and Rice University, and the CTP7, developed by the University of Wisconsin. Table 4.1 shows some of the major specifications weighed when making the decision on which board to choose. Number of high speed optical communication links were important in order to support communication to as many chambers as possible per AMC. The FPGA power and RAM determined how much logic the boards could produce in order to support more connections as well.

Another major factor in the choice of AMC was time. The board(s) needed to be ready to be installed in the Slice Test at the end of 2016. This would require both firmware and software development in advance to handle the addition of a new board. Because of this requirement and many others, the collaboration decided to use the CTP7 board for the upgrade. Several CTP7 boards were available for testing and development purposes, and the designers were helpful in debugging problems with integrating the board into the GEM DAQ system. This allowed for fast development in 2016 to prepare for the Slice Test.

4.1 GEM Online Software

The GEM DAQ system online software runs using the XDAQ middleware, the basis of all CMS online software [14]. This software controls data-taking from the detectors, as well as facilitating hardware access, communication protocols, services, etc. from the electronics. The GEM online software suite includes hardware managers, monitoring and

Figure 4.1: CTP7 Board, the chosen AMC for the GE1/1 Upgrade

alarming tools, the GEM supervisor, and different calibration scan routines.

4.1.1 Scan and Calibration Routines

Several calibration scan routines have been implemented in the GEM online software. These scans are useful to adjust parameters which depend on the location and configuration of the chamber and electronics. Moving chambers, exchanging optical fibers, switching electronics boards, and many other common actions can completely change the system performance. Performance also varies across hardware and must be calibrated to account for imperfections introduced during production. Integrated scan routines allow these variables to not affect the ability of the electronics to successfully take data. These scan routines will be introduced in this section, and their results will be detailed further in Chapter 5.

Threshold Scan

Each of the front-end VFAT chips on every detector has a configurable threshold. This threshold value is mapped to the comparator in the chip and determines the point at which a detected charge level on a strip is considered a muon hit. If the threshold is too low, background noise in the detector electronics may cause false hits. If the threshold is too high, actual muon hits may not deposit enough charge to register a hit in the chip and will be missed. Either of these situation drastically reduces the efficiency of the detector. Thus, the threshold for each chip and each channel must be scanned in order to select the optimal value.

This scan is done channel-by-channel by firmware on the OH for each chip in parallel. The threshold is set by writing to a digital register, which is then converted to an analog value by the VFAT. Then, random triggers are sent to see how the VFATs respond at each threshold.

The scan begins by setting a full chip or specific channel to its lowest threshold value, which is a digital value of 0. This essentially means there is no threshold, so that any level of charge registers as a hit for each strip. This causes the chip to respond with hits in every channel almost constantly with each trigger. The threshold is increased slowly, recording hits received for each channel. Once the threshold hits a certain value, the background noise present in the chamber is filtered out, and each channel stops responding to triggers. The point at which each channel stops responding varies, so the optimal threshold value differs for each channel. The threshold is continually raised until it is very high, where no channels ever respond with hits. When the number of hits for each channel is plotted versus the threshold, a curve is formed. This curve starts at maximum, and then rapidly drops off at a certain point. This point determines the optimal threshold to set each channel. These points are recorded for every chip and channel in the chamber, and the thresholds are set

accordingly.

S-Curve Scan

At a particular threshold, the VFAT response depends directly on the injected charge pulse magnitude. Using an analog-to-digital converter (ADC) located on the OptoHybrid, an injected calibration pulse and the associated response of the VFAT can be measured. This relationship is plotted in an s-curve, shown in Fig. 4.2, which shows the response of the VFAT, measured in hits-to-events ratio, as a function of the calibration pulse height. The resulting curve starts at zero for low calibration pulse heights, when the VFAT has no response, and turns on to one at a certain calibration pulse height, when every event registers a hit. This curve can also be recorded for each channel, which is an effective way to check uniformity across channels. The s-curve can be used to characterize many analog characteristics including noise, threshold, dynamic range, and linearity [10].

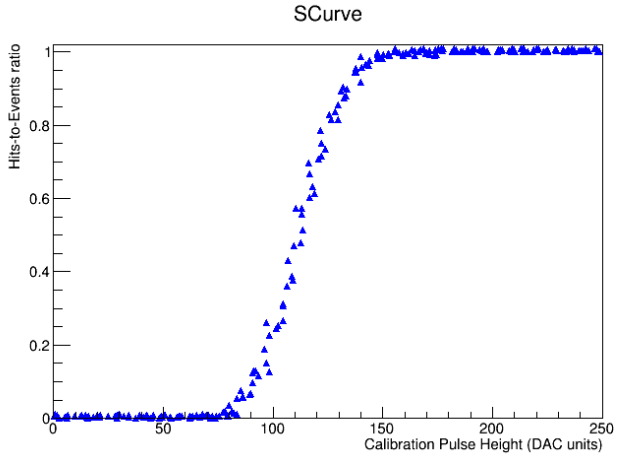

Figure 4.2: Typical s-curve for a single channel

The measured s-curve of each channel can be fit with a logistic function of the form in Eq. 4.1, where x_0 is the midpoint, or turn-on, and σ is the steepness of the turn-on

slope. These extracted parameters can then be used to set the trimDAC register. This register changes the threshold slightly for each channel to adjust for statistical fluctuations from fabrication [10]. In summary, the threshold scan is taken to set an appropriate coarse threshold value for each VFAT, and then the s-curve scan is performed to equalize all channels for each VFAT.

$$f(x) = \frac{1}{1 + e^{-\sigma(x-x_0)}} \tag{4.1}$$

Latency Scan

The GEM DAQ electronics are constantly producing trigger data which is sent to the trigger system in CMS. This trigger decision decides if the DAQ system should store its full-granularity tracking data or not. As the trigger decision is being made, the data is placed in firmware buffers for a small amount of time waiting before sending it offline to be stored. When the trigger decision is received, the data from the event indicated by the trigger must be saved. The trigger decision has a fixed latency, which depends on the distance the trigger data must travel in the system. Therefore, in order to save the tracking data for the correct, triggered, event, this latency must be calculated. Latency is defined as the number of clock cycles that it takes for the electronics to receive the L1A trigger signal from the trigger system after sending trigger data. This latency is a very small amount of time, so small changes such as swapping fibers with different lengths and placing the chambers further away from the trigger path can affect this latency significantly.

The latency scan is done by sending calibration pulses to the chamber and waiting to see when a response is received. This can vary based on running modes and other triggering conditions, so the latency scan is important to perform before data-taking for any new configuration. A calibration pulse is sent to the chamber, resulting in a guaranteed hit which will be sent as trigger data. A trigger decision, or L1A signal, is received a small

time later (around 35 clock cycles or 875 ns for the Texas A&M test stand). The firmware takes the time that the L1A was received, then counts backwards a single clock cycle at a time to see when the trigger data for that event was fired from the chamber. The difference between the fired event and the received trigger signal is the latency of the system. This latency can be measured repeatedly to get a very accurate measurement in order to choose the optimal value to match as many events with the proper L1A as possible.

4.1.2 Hardware Managers

Each of the major electronics (VFAT, OptoHybrid, CTP7, AMC13) has its own software manager built into the XDAQ system. These managers provide direct access to the FPGA located on the boards via IPBus protocol. They allow experts to read and write dozens of registers to check statuses, flags, error counters, and other information from the XDAQ data-taking application.

4.1.3 GEM Supervisor

In order to begin a data-taking run, all of the hardware components must be in-sync with one another and placed in the correct software and firmware state for data-taking. This is done through a system manager in software called the GEM Supervisor. It is in charge of controlling all of the individual hardware managers and keeping them synchronized with the overall system state. This supervisor vastly simplifies the data-taking process, and allows the user to not have to worry about the individual DAQ components.

4.2 WebDAQ

A useful online tool, referred to as the WebDAQ, is an online web application to actively monitor and control the GEM DAQ system. The WebDAQ also integrates various scan routines, control interfaces, and a data quality monitoring (DQM) interface [21]. The WebDAQ application replaces an earlier control and monitoring application based on Py-

Chips, which facilitated hardware access through several Python scripts. These scripts were each developed to do a specific task and needed to be run repeatedly, which is infeasible for a large DAQ system. The WebDAQ system implements an improved architecture using more dynamic infrastructures.

4.3 Data Quality Monitoring Software

Data quality monitoring (DQM) software is a common tool for monitoring detector systems in CMS. There is a central DQM framework which is used to control the CMS detector during data-taking and validate the recorded data as usable for physics analysis. [15] This system includes structure for booking, filling, and archiving histograms and monitor elements, and performing automatic quality tests.

4.3.1 WebDAQ DQM

As mentioned previously, the WebDAQ tool includes a built-in DQM interface. This allow users to check the consistency of the recorded data and even change parameters of the run if necessary. The DQM in this application is primarily used for quick monitoring of data without storing it. In order to store the full raw data stream and process it offline in-depth, a separate data quality monitoring software has been developed for the GEM DAQ system.

4.3.2 GEM Light DQM

The GEM Light DQM system to be run online was intended to be a lighter version of the central GEM DQM designed for offline validation of the previously taken data. It was developed in parallel with the electronics themselves, so it was made to assist with expert debugging of the system as well as the original functions of DQM software. To differentiate the GEM DQM from the central DQM, the term "Light" or "Local" was assigned to it. Assume from this point on that DQM is referring to this "Light" DQM developed for the

GEM DAQ system, and not the GEM part of central DQM of CMS, which has yet to be developed.

The GEM Light DQM software is the primary development of the current thesis work. It is written using a combination of C++ and Python, while operating from a database using Oracle [**?**] and a web browser run with HTML/CSS assisted by Django [18]. It was initially created as a fully offline tool. Data was taken and stored in large binary files to be separately input into the DQM software for processing. In order to make this an online process which could run while data was being taken, chunking was implemented. Instead of waiting for data-taking to stop, smaller output files (chunks) are produced after a certain number of events are collected. This allows the DQM software to simultaneously process data files while new ones are being collected. This naturally introduces some latency into the process, but if the DQM software is able to process a single data file (chunk) as fast as it is produced, the system can be considered online. To reiterate, "online" in the case of DQM is defined as the software processing and displaying data as fast as it is produced. The following sections will step through the DQM process, illustrated in Fig. 4.3.

4.3.3 Unpacker Module

When a single data-file, or chunk, is output by the DAQ system, it is stored as a binary file with a .dat file extension. The data contained within the file is stored following the CMS common data format, shown in Fig. 4.4. This event block data format divides the data into header, payload, and trailer sections. The event header identifies the event type, LV1 trigger ID, bunch crossing ID, and other information which describe exactly when the event happened for matching with other events around CMS. The payload block begins by identifying the AMCs included in the event block followed by the individual payloads from each AMC. These payloads each have their own individual data format as well. Finally, the trailer contains cyclic redundancy checks (CRC) for validation and data

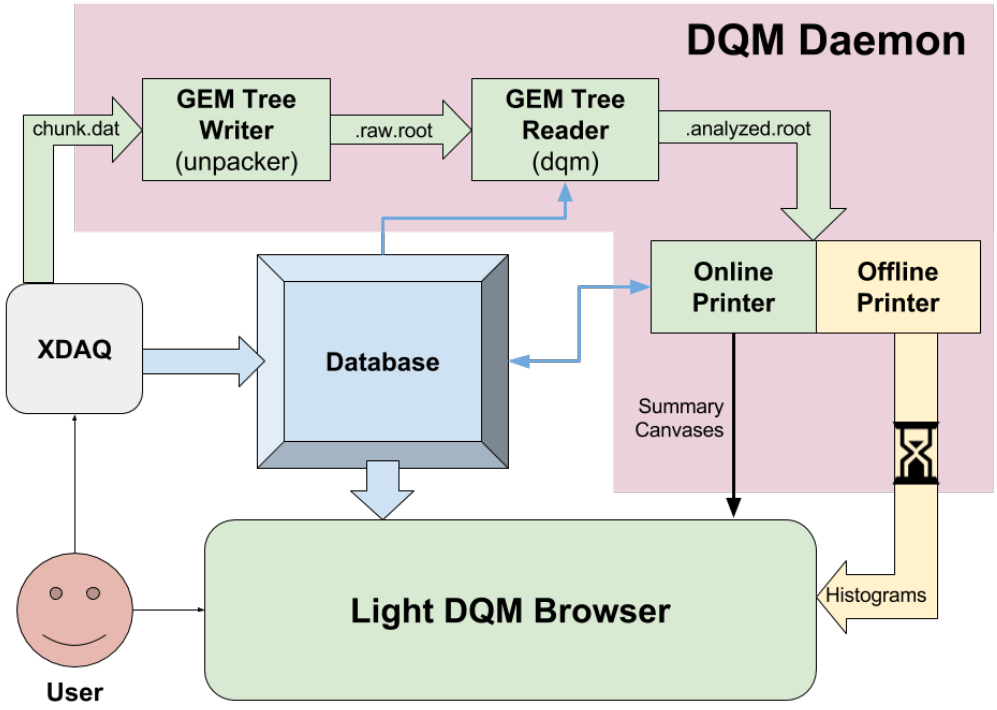

Figure 4.3: Overview of data quality monitoring software process

corruption detection among other information.

The unpacker module converts this binary information into a more accessible format using the CERN ROOT framework [16]. As stated in the user guide, ROOT is an object-oriented framework aimed at solving the data analysis challenges of high-energy physics. It provides methods of storing large amounts of information into an easily-accessible and manageable format. The GEM DQM unpacker module stores all of the information contained in the data file in a ROOT tree event-by-event. Trees are a convenient way of storing the event data, due to the "tree-like" quality of the GEM DAQ system. The event itself is the trunk of the tree, containing all the information about the event as a whole, including all of the hardware branches. Each branch represents a single piece of hardware, and contains all the information about that hardware element in "leaves" off of the branch. Starting

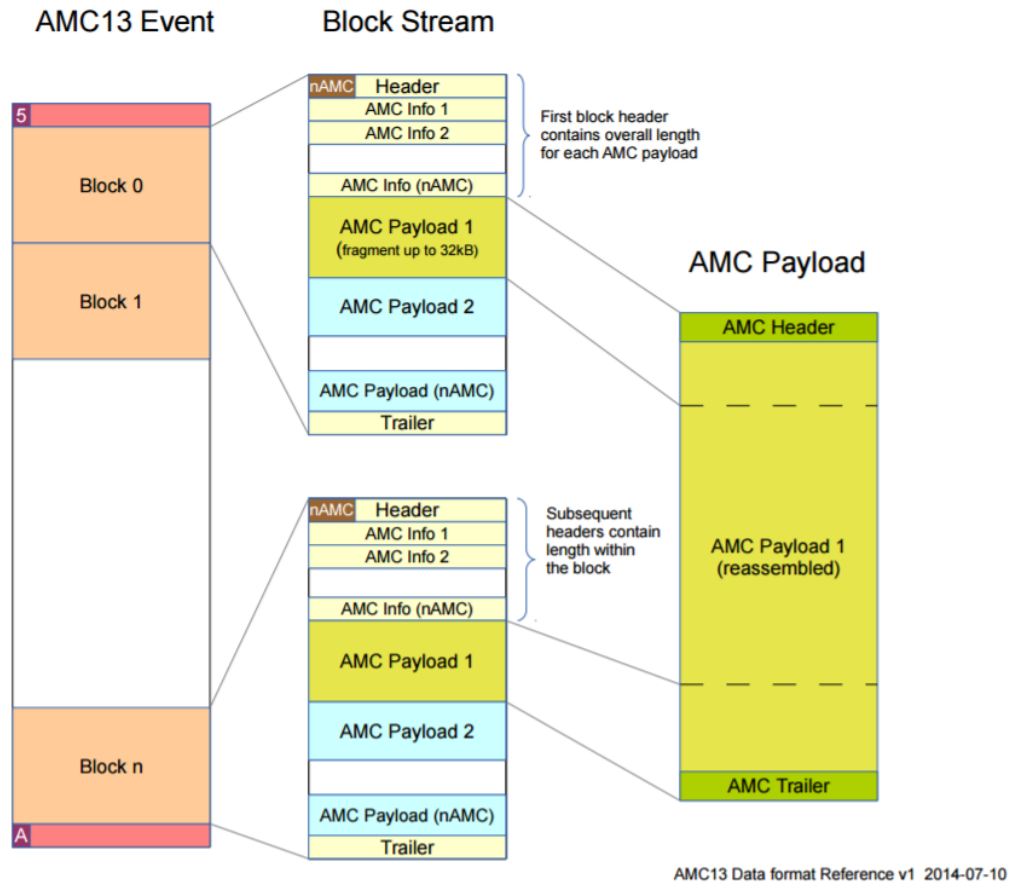

Figure 4.4: Data Format as sent to DAQ PC from AMC13

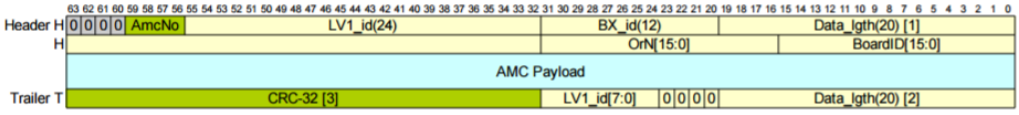

Figure 4.5: Data Format as delivered by OptoHybrid to AMC firmware

with the AMC13, each piece of hardware connects to the numerous elements below it in the system. Thus each branch can store the leaves of information about itself and branch off to the next level, all the way to the front-end VFAT chips. The information in the tree is still the raw data in a different format, meaning no analysis has been done yet. Thus, the

unpacker module outputs this tree as a "raw" ROOT file with the .raw.root file extension. This raw ROOT file is then passed to the GEM tree reader module.

4.3.4 Tree Reader Module

In order to monitor the system and validate the received data, several histograms are created to look for expected qualities in the data and indicate problems. The GEM tree reader module does this by taking the raw ROOT file produced by the unpacker module containing the ROOT tree and looping over all of its data. Utilizing the efficiency of the ROOT tree and C++ optimization makes this process very fast, so that more events can be processed in less time.

The tree reader module first iterates over all of the events stored within the file. Each event is its own tree containing branches of information, as detailed in the previous section. For example, the first branch off of the main event tree is the AMC13. This branch includes all of the AMC13-specific information contained within that event, as well as each of the AMCs connected to the AMC13 as branches. Each of those AMC branches contains the AMC-specific information and chamber branches, etc. The code to loop over the entire event uses a nested for-loop to place all of the event information into vectors for further analysis.

Event tree processing is highly parallelable, because every event is completely independent from one another. Thus, this process is sped up using the PROOF ROOT framework [17]. This framework allows the tree reader module to run the analysis in multithread or multicore mode both locally on a single computer and on a data analysis computer cluster.

Once all of the events have been processed and analyzed, and the information has been stored into vectors, histogram production begins. Hundreds of histogram objects are created, depending on the amount of hardware included in the data run. These histograms

are created and filled using the ROOT framework, integrated into C++.

4.3.5 Printer Module

The GEM DQM printer module takes the histograms produced by the tree reader module and exports them to printable formats. This allows the histograms to be displayed in the DQM web browser and viewed by programs outside of ROOT. Each extra file format used doubles the number of files to produce, which slows the DQM process down significantly. Therefore, the only format currently produced is JSON (JavaScript Object Notation), which is the format used in the DQM web browser. This format allows the histograms to be interactive in the browser, which will be detailed further in upcoming sections.

4.3.6 Daemon

Daemon, in computing, is defined as a computer program that runs as a background process, rather than being under the direct control of an interactive user. A DQM Daemon, written in Python, initiates and facilitates passing files between steps of the DQM process. This allows the DQM process to be fully automated and, if fast enough, fully online.

When the daemon is started, it immediately begins searching for files to process. It looks for data files (in chunks) in a specified location, normally wherever the XDAQ is outputting the data files. When one is found for the first time, it passes the name of this file to the unpacker. The output file produced by the unpacker module is immediately passed to the tree reader module. The output of the tree reader module is a root file containing all of the DQM histograms and summary canvases. Finally, the histograms produced by the tree reader module are passed to the printer module and the printed histograms are stored in a location which will later be accessed by the DQM web browser. All of these steps are done through command line calls using the subprocess library in Python. Once it takes a chunk through the full DQM process, the daemon then moves on to the next chunk.

If the DQM were to act on every data chunk output by the system completely separately, it would output separate histogram images for every chunk. Chunks are relatively small in number of events, so there are often thousands of chunks produced per data run. Therefore, the DQM needs a way of combining the information of each chunk so that the final output of the system is the combination of the data from the entire run, rather than an individual chunk.

A key feature of using ROOT to produce the histograms is that ROOT provides fast methods of combining histograms from different files. This step is built into the DQM daemon. Between the tree reader and printer modules, the DQM daemon takes the chunk it is processing and combines the histograms (in ROOT format) with the combined ROOT file containing all chunks processed up to this point. This combination ROOT file afterward contains all of the data produced in the run, including the most recent chunk. This is the file which is then passed to the printer module. This results in the histograms printed to contain all of the data produced by the entire data run. When new chunks are processed and combined, the new printed histograms replace the old ones, so that only the most recent and complete data is shown in the web browser.

4.3.7 Database

It would be difficult and inefficient to maintain all of the information about a run within local memory or the data itself. A centralized database is needed to store this information. The database keeps track of hardware configuration, hardware state, run type, run number, location, and date. Another feature of keeping all of the runs in a single database is that they can easily be compared and accessed from anywhere through the DQM web browser. This can allow experts to track hardware performance, find behavioral patterns in the system, and more intelligently debug issues.

4.4 DQM Web Browser

The ultimate feature of the DQM system is its online web browser. It is capable of accessing every run ever taken (as long as it is put into the central database) from anywhere with Internet access. Furthermore, it is able to monitor a data run in real time to display key information about the quality of data being produced for rapid on-the-flight debugging. The browser was designed to be intuitive and user-friendly so that non-GEM DAQ experts would be able to use it effectively without understanding the full DQM process. The browser is effectively just a medium for viewing the information stored in the database and histograms produced by the DQM in an interactive way.

It is run with the help of Django [18], an open-source Python Web framework. Django facilitates and displays the browser using high-level coding (Python) integrated with the HTML/CSS that defines web-pages. The browser is run from a central location and then can be accessed using a specific host and port from any standard Internet browser. The following sections will walk through the browser and how it is used.

Run List and Run View

When the DQM web browser is initially opened, it displays the Run List, shown in Fig. 4.6. This list contains every run found in the database, sorted by date. It displays the run number, station location, date, and period. This list can be toggled from the top menu bar "Run List" button in blue at any time to select a different run. Once a run has been selected, the run list collapses to the left sidebar and the page opens up the run view for the selected run.

The run view, shown in Fig. 4.7, displays all chambers present in the hardware configuration stored in the database for the selected run. The page header shows information about the current run being displayed: station location (CERN904) and run number (000047). In the example shown, there is only a single chamber being displayed, however the table is

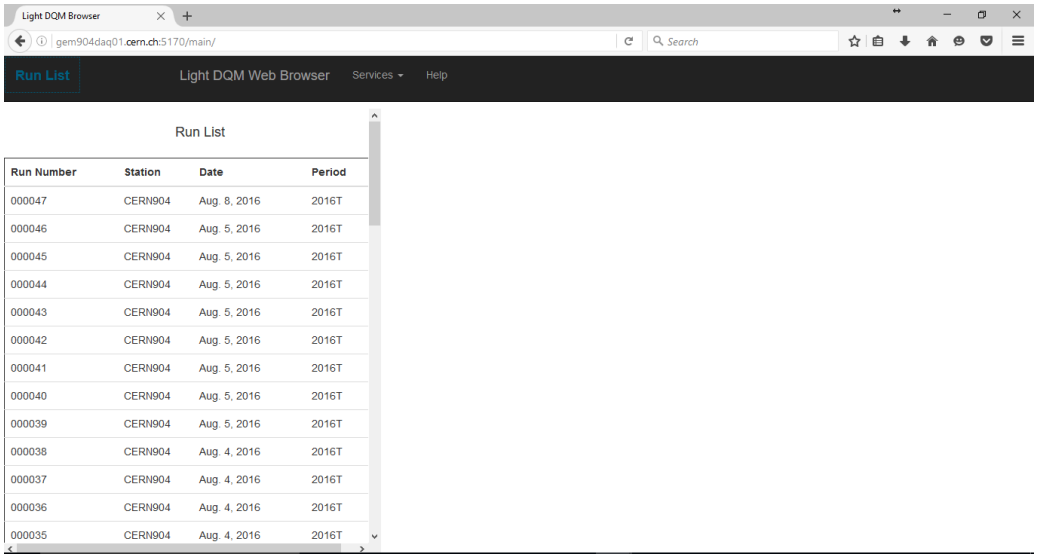

Figure 4.6: An illustration of the Light DQM Run List Panel displayed when initially accessing DQM web browser

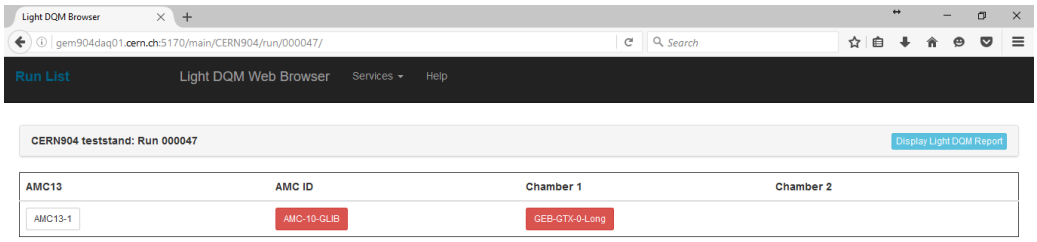

Figure 4.7: An illustration of the Light DQM Run View once specific data run has been selected

fully scalable to account for any number of chambers in a run. Django handles the display so that the table is automatically scaled and filled based on the information pulled from

the database.

Two chambers make up a single super-chamber, and multiple of these super-chambers can be connected to a single AMC. Multiple AMCs are connected to one AMC13, with a single AMC13 able to handle the full GEM system. This is reflected in the chamber table. When additional chambers are added to the system, they will be listed as super-chamber pairs next to their respective AMC. Clicking a chamber button navigates to the chamber view.

Chamber View

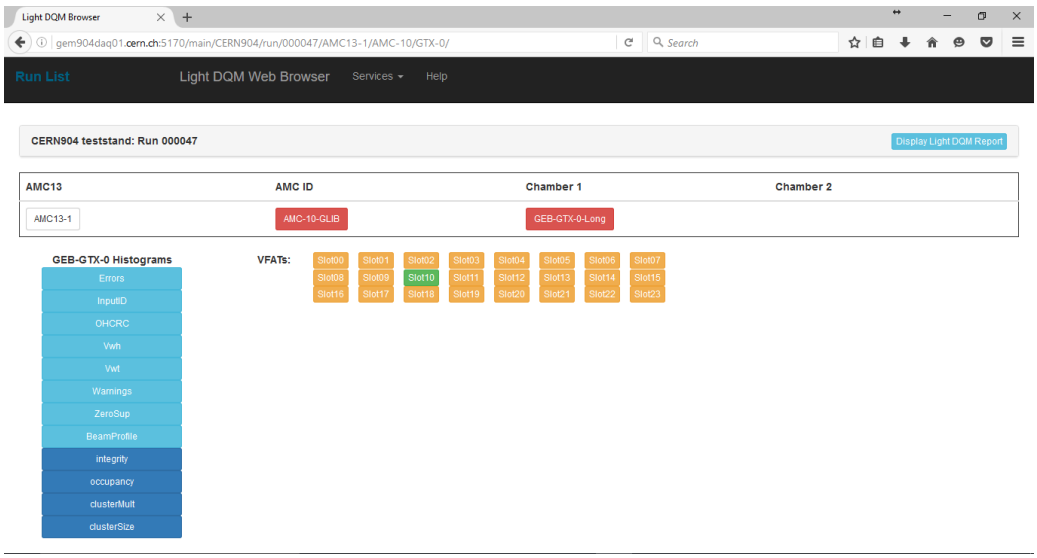

Figure 4.8: An illustration of the Light DQM chamber-specific histogram types (light blue buttons on left) including summary canvases (dark blue buttons)

The chamber view, shown in Fig. 4.8, displays the chamber-specific histograms, summary canvases, and front-end VFAT-chip buttons. Each chamber has up to 24 VFATs connected to it, reflected in the buttons organized into 3 rows similar to their layout on a chamber. VFAT buttons are only enabled (and colored) if the hardware configuration

indicates that they were connected during the run.

The chamber-specific histograms can be selected to display histograms filled only with data from the selected chamber. This provides detailed information that experts can use to see the performance of a single chamber and debug problems. Specific examples will be detailed in future sections. Summary canvases are specific to a single chamber, and are discussed further in the next section.

Summary Canvases

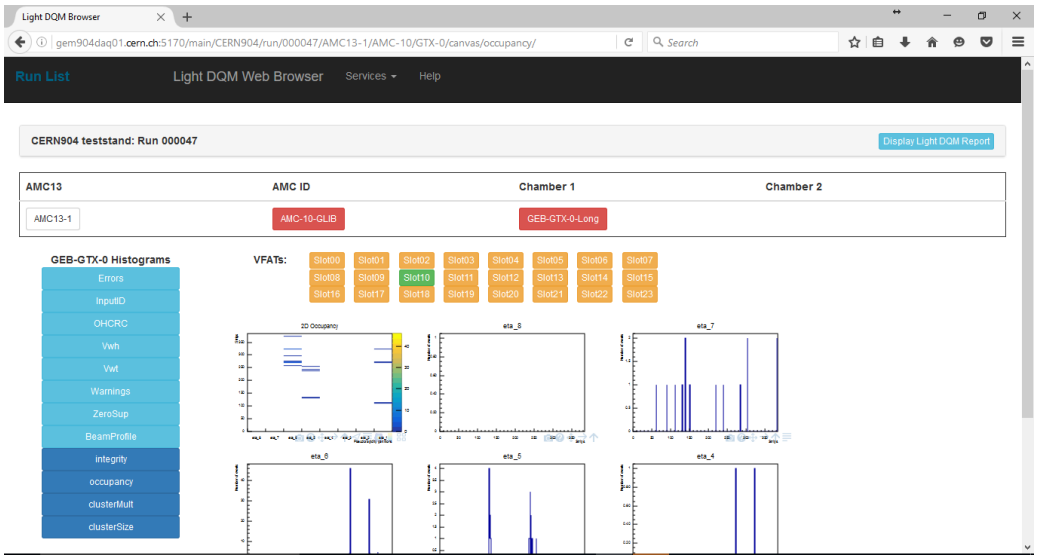

Figure 4.9: An illustration of a displayed Light DQM summary canvas for a single chamber

Summary canvases provide the most essential information in verifying that chambers are working as expected. As mentioned previously, the DQM software is not capable of processing all of the histograms in real-time. The summary canvases alone, however, can be processed fast enough to display them as fast as data is being taken. When rates are sufficiently low, the summary canvases are fully online. If rates exceed maximum

capabilities, the events are sampled in order to produce histograms from a fraction of the events.

There are currently four different summary canvases: integrity, occupancy, cluster multiplicity, and cluster size. The integrity summary canvas summarizes the validity of the individual data packets themselves. Firstly, it provides a check of the VFAT response uniformity. For every trigger sent to a chamber, every connected VFAT is expected to respond with a data packet. If a VFAT is not responding to each trigger, that is an indication of a problem. Control bits are included in the data stream. These are constant values which should be the same for every data packet. If one of these control bits is incorrect, this indicates a major problem with the data packet formation or transmission. A cyclic redundancy check (CRC) is also performed on each data packet sent from the VFATs. This check protects from single-event upsets (SEU) and other data corruptions. If the CRC value sent in the data packet does not match the recalculated CRC in the OptoHybrid, it indicates possible data corruption at this stage. In conclusion, the integrity summary canvas is used to indicate possible electronic inefficiencies, where data may be lost or corrupted.

The occupancy summary canvas displays the GEM readout board strips that registered hits. During normal operation, a hit would indicate that this strip was the location of a hit by a muon or other charged particle. The histograms themselves are divided into one full beam profile, which shows all of the strips in a single plot, and 8 other eta-partition histograms. Each GEM chamber covers 8 different eta-partitions, so it can be useful to view the hits based on these partitions. The occupancy summary canvas can indicate both dead and hot channels very easily. A dead channel means one that never provides a hit, even when it should. Conversely, a hot channel always registers a hit, even with no charge deposited in the readout strip (no real hit). Dead channels are seen clearly during test beams, where a clear spike in a region of strips is expected. Holes in this area indicate channels that are not responding when they should be. Hot channels can be seen in any

operation as huge spikes in the occupancy plots for single strips. No strip should statically be hit every time, so this is clearly an indication of an electronic problem.

When a muon passes through the detector, it will often deposit charge on more than a single strip. This small collection of strips which all respond to the same muon hit is called a 'cluster'. The cluster multiplicity summary histogram displays the number of clusters registered for each bunch crossing. Statistics dictates the expected number of clusters per bunch crossing, so deviations from the expectation indicate problems. The cluster size summary canvases display the number of strips registered in each cluster. If clusters are too large, meaning more than about 2 or 3 strips are registered per cluster, than this indicates a problem with either the electronics or the GEM chamber. Similar to the occupancy summary canvas, these canvases also display the distributions for the entire chamber, as well as each of 8 eta-partitions for a total of 9 histograms.

Hardware Histograms

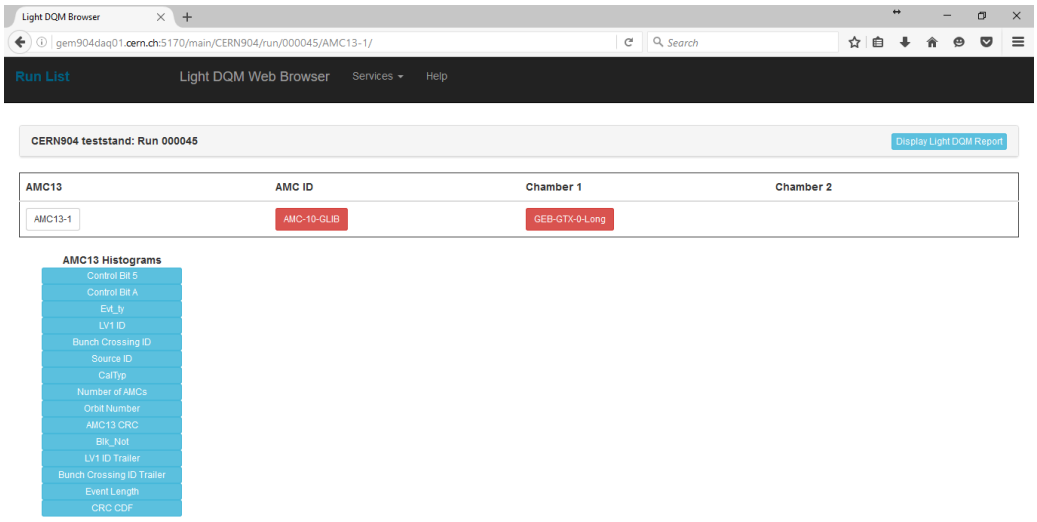

Figure 4.10: An illustration of the Light DQM AMC13-specific histogram list (buttons shown on left)

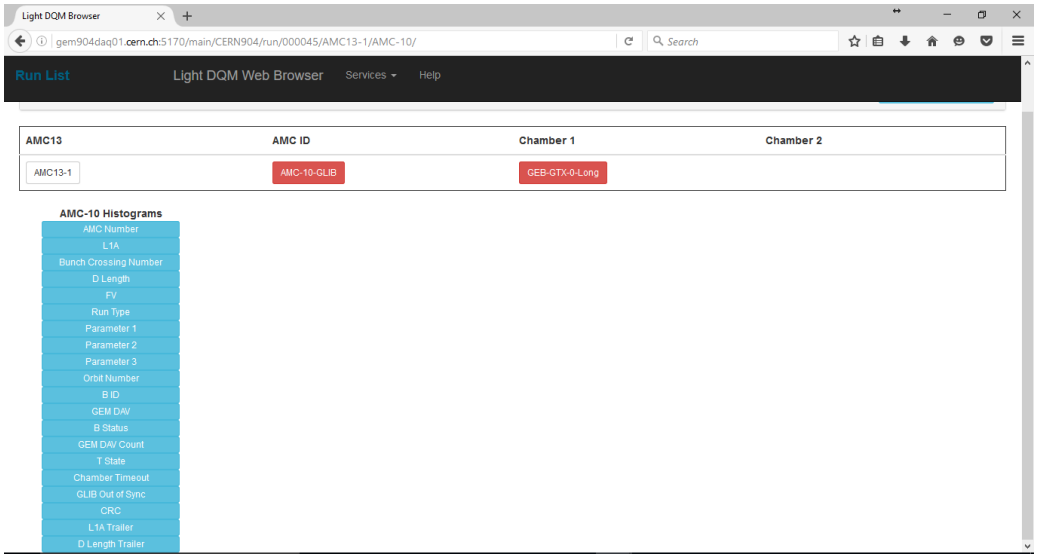

Figure 4.11: An illustration of the Light DQM AMC-specific histogram list (buttons shown on left)

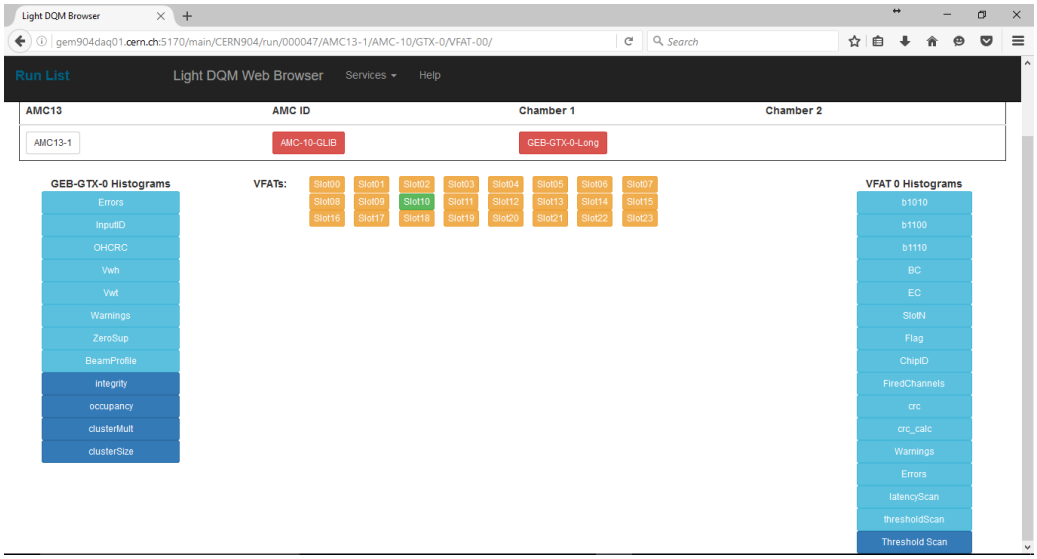

Figure 4.12: An illustration of the Light DQM VFAT-specific histogram list (light blue buttons on right) and chamber-specific histogram list (light blue buttons on left)

All other hardware-specific histograms are included in the "offline" DQM. Once a run has been fully taken, the data is processed to produce every histogram. There are histograms specific to every level of hardware in the GEM DAQ system. These histograms are shown by clicking on the desired hardware button. Examples of the AMC13-specific histograms are shown in Fig. 4.10, AMC-specific histograms in Fig. 4.11, and VFAT-specific histograms in 4.12. OptoHybrid and GEB-specific histograms are both included with the chamber-specific histograms, because these are always matched one-to-one for version 2 electronics.

4.5 Expert Tools

In developing the DAQ system, experts often need lower level tools in order to access all the information available from specific parts of the system. These tools are specialized and made by experts with specific needs in mind. The following sections outline some of these tools.

4.5.1 CTP7 Command-Line Interface

When the CTP7 board, the chosen AMC to be used by the GEM DAQ system, was first introduced, there were not very many tools available to assist developers. An online hardware manager did not exist, so many developer functions were unavailable. For example, when developing firmware for the board, it is very common to read and write registers in the board's field-programmable gate array (FPGA) to test certain features and monitor statuses. Originally, reading and writing registers required a developer to find the exact address in memory (8 hexadecimal characters) that they wanted to read from or write to, and type out a full command with this address. This was quite time-consuming and unnecessary. A command-line interface was thus developed, as part of the current thesis work, in order to improve this action.

The main goal of the CTP7 command-line interface is to provide a quick method to

read and write registers from the board's FPGA to assist developers. The tool was written using the Python 'cmd' library [19]. This library provides a framework for processing user input and includes helper functions for extra features. It was originally designed to run on the ZYNQ system-on-chip (SoC) running a Linux kernel. The tool is thus running on the CTP7 board itself, allowing for faster reading and writing operations via the AXI bus between the Zynq SoC and the board's FPGA, rather than from a separate DAQ computer connected to the GEM electronics. In the future, read and write operations will also use remote procedure calls (RPC). These improvements will be discussed further in Chapter 6.

4.5.2 CTP7 Monitoring Page

The CTP7 board was introduced to the GEM DAQ system after primary development of previously outlined monitoring applications. Furthermore, it is extensive and physically unique enough to warrant its own independent monitoring application. This application has been developed to take advantage of the on-board ZYNQ SoC. The CTP7 monitoring tool has been developed on top of the command-line interface to allow experts to actively monitor key registers automatically. It uses the same Django framework as the Light DQM Browser discussed previously. Read and write operations utilize the same library as the command-line interface. The home page, shown in Fig. 4.13, displays the status of the CTP7 divided into separate modules.

The DAQ module displays key register statuses associated with data-taking. These include counters and flags which indicate problems such as buffer overflows. The TTC module displays triggering and timing information, including stability of the clock and rate of L1A triggers received. The Trigger module displays information about the trigger data being received by the connected OptoHybrids. Finally, the OH module displays the status of connected OptoHybrids. As shown in the example, only OH0 is currently connected

properly. Separate pages allow for read and writing of registers, a more user-friendly approach to the command-line interface functionality.

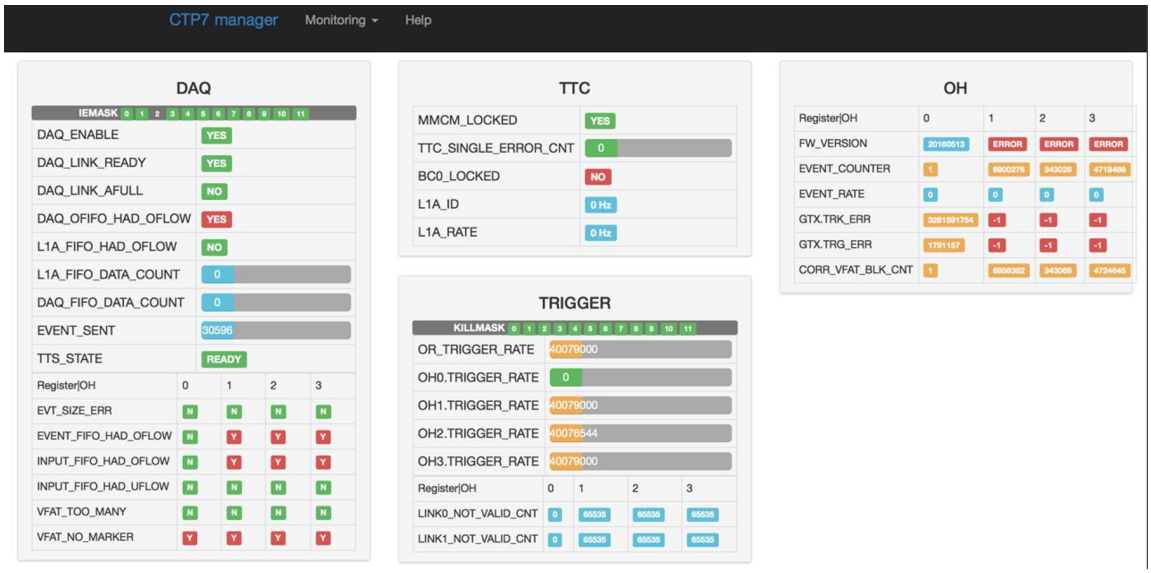

Figure 4.13: CTP7 Monitoring Application home page - one OptoHybrid connected

4.5.3 CTP7 SBit Scan

Select bits, or SBits, are the raw trigger data sent from each VFAT and packaged by the OptoHybrid which indicate the area where a muon hit occured. This information is part of the trigger data and not included in the tracking data read out by the DAQ system. Therefore, it is never saved, making it difficult to analyze and verify. The CTP7 SBit scan has been developed as part of the current thesis work to verify that each SBit is encoded and sent properly for each VFAT. It turns on a single channel (of the 128 channels per VFAT) at a time, sends a configurable number of calibration pulses, and verifies that the correct number of SBit "triggers" are seen by the CTP7. It then checks that these SBits are correct by verifying that their encoding matched the active channel. It can identify problems with

soldering on Panasonic and/or Samtek connectors which transmit SBit signals, VFAT/GEB problems, and firmware bugs, making this an important scan to run during the chamber production process.

The SBits consist of 8 bits per VFAT, which are then transmitted to the OptoHybrid through debugging headers in the data format. The OptoHybrid firmware takes each of the 8 bit clusters and logic ORs them, resulting in 24 total bits of information. These 24 bits are turned into 6 bits through a programmable selection mechanism and transmitted to the CTP7. The SBits are not saved, but rather stored momentarily in a debugging register on the CTP7. Every data packet received by the OptoHybrids update these SBit debugging registers. This makes analysis of the SBits somewhat tricky.

The full process of the SBit scan is illustrated in Fig. 4.14. It consists of two parts: scanning and mapping. The scanning part of the test verifies that the CTP7 receives the correct number of triggers for a certain number of calibration pulses. Naturally, each calibration pulse should result in a single trigger, which is measured by reading a trigger counter register on the CTP7. If more triggers are received than sent calibration pulses, this can indicate a hot or noisy channel. If no triggers are received, this can indicate a dead channel or bad connection. The scan begins by resetting the trigger counts and then verifying that they returned to zero. If they did not, this indicates that the channel is hot, meaning it is continuously outputting triggers.

The mapping part of the SBit scan verifies that the SBits were encoded properly. The SBit sent from each OptoHybrid contains 15 bits which encode the VFAT, location, and size of the cluster received during that BX. The script sends calibration pulses repeatedly to a specific strip and VFAT on the chamber. As the script sends calibration pulses to specific channels, it verifies that the encoded location for each SBit received matches the location of the sent calibration pulse. The received SBits are only stored in debugging registers for a short period of time once received. Therefore, reading the register does not

necessarily guarantee that an SBit will be read out. The scan gets around this issue by reading the debugging registers multiple times until an SBit is read out.

The results of both parts of the scan are recorded to an output text file. The scanning part records expected versus received SBits values, hot channels, and other debugging information. With the GEB version 2, it also maps the hot channels to their connector on the GEB so that they can be checked for soldering mistakes.

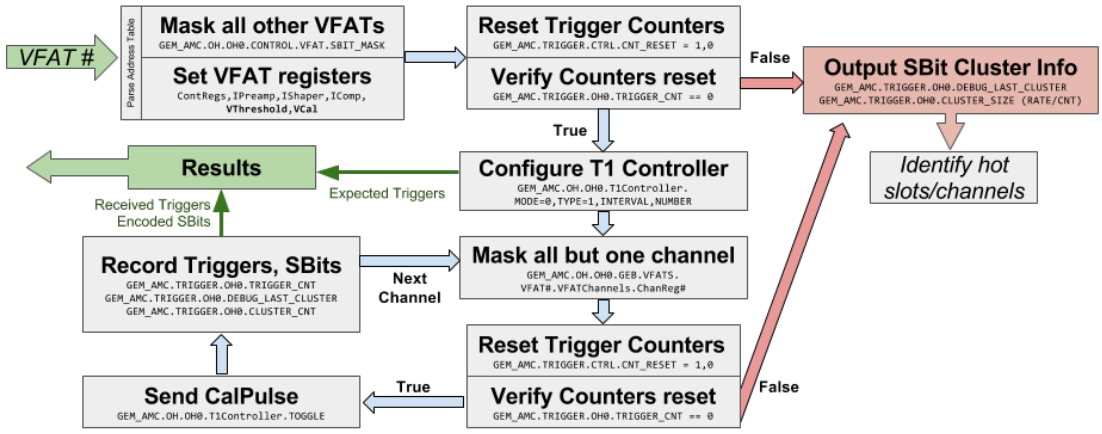

Figure 4.14: SBit Scan Flowchart

CHAPTER 5

PERFORMANCE OF THE GEM DAQ MONITORING SYSTEM

This chapter will explore the different use-cases and results of the GEM DAQ monitoring system. Various elements of the system have been deployed to multiple test stands for development. The results from these test stands on the different parts of the GEM DAQ system will be shown, illustrating performace of the monitoring applications and primary software developments that make up this thesis work.

5.1 Electronics Test Stands

The GEM collaboration has various test stands around the world. They can be classified as development, integration, or production test stands. Development test stands often have various elements of the GEM DAQ electronics, but not necessarily the full system. They are used to develop hardware, firmware, and software without the GEM chambers themselves. There are currently development test stands at Texas A&M University (College Station, USA), Universite libre de Bruxelles (Brussels, Belgium), Rice University (Houston, USA), and a few other locations. Another key development test stand is located in building 904 at CERN, also referred to as b904. Building 904 does, however, have GEM chambers, so it is capable of taking cosmic data measurements and performing other tests which require a GEM chamber.

The integration test stand is where GEM chambers are tested before being transferred to Point 5, to be installed underground in CMS. This location is a clean room which performs all quality control steps to verify that each chamber is acceptable for use in the CMS

detector. The integration test stand was originally located at the tracker integration facility (TIF), however it has moved to building 904.

The production test stand is located at Point 5, underground in the CMS detector. This is the final installation location where chambers are placed to take data for the experiment. Ten GEM chambers (five super-chambers) have been installed for the Slice Test so far. The rest of the GEM chambers are planned to be installed at the production test stand in 2019 during the second Long Shutdown (LS2) of the LHC.

Most development test stands have between one and three GEM chambers (or their electronic equivalents). This is relatively easy to manage in terms of data storage and manipulation. The GEM Light DQM software simplifies this process, but is not absolutely essential. The integration test stand can have up to a dozen or more chambers, many taking data in the cosmic stand at the same time. This many chambers all producing data is difficult to manage, and data analysis is greatly assisted by the GEM Light DQM software and web browser. The on-going Slice Test has 5 super-chambers (10 chambers), and will thus benefit greatly from installation of the Light DQM software following commissioning and calibration once the chambers begin to take real data. The final GE1/1 system will have a total of 72 chambers in each CMS endcap all producing data and requiring data monitoring and validation. This is when the software outlined in this thesis work will truly become essential.

5.2 Test Beam

Multiple test beams have been organized since the inception of the CMS GEM system to test the detector performance [20]. The GE1/1 prototype detectors were tested at CERN and Fermi Lab in two initial test beams in 2012 and 2013. These test beams were primarily to test the performance and efficiency of the detectors themselves, and less focused on the DAQ electronics system. Two more test beams were later organized in Fall 2014 and 2015

in order to begin testing the performance of the detectors with a new DAQ architecture.

The test beams consisted of 150 GeV pions and muons. The November 2015 test beam employed two GEM detectors using version 2 electronics, shown in Fig. 5.1. Each GEM chamber used GEB v2, OptoHybrid v2a, and VFAT2s. Both detectors were only partially filled with VFAT2s, filling the 4 central slots of each column on each GEB. One GLIB was used to read out both OptoHybrids. For better analysis, the detectors were positioned so that the beams would pass through a single VFAT2 region on the detector. Triggers were provided by the coincidence of four scintillators, three in front of the GEM chambers and one behind them.

Data was taken and analyzed offline using the DQM software for various different system parameters, including high-voltage level, front-end threshold, and trigger rate. The full light DQM in its current form was not available during the 2015 test beam, however the offline data saved can now be processed and allows a good illustration of the light DQM capabilities.

5.2.1 Initial Calibration Scans

Before the beam is turned on, threshold scans are taken to calculate the noise level and set the optimal threshold value on the VFAT2s for both chambers. Fig. 5.2 shows the threshold scans taken using the WebDAQ application for the test beam. Threshold scan curves are expected to drop all the way to zero at a certain value, so the large tails on both plots indicates a significant source of noise on both chambers which is unable to be canceled by setting a large threshold. After seeing the results of these scans, the thresholds are set to 25 for both chambers for the rest of the test beam, and a thorough noise investigation is launched which discovers several configuration issues following the test beam.

Next, a latency scan is taken to calibrate the timing of the trigger data path. The

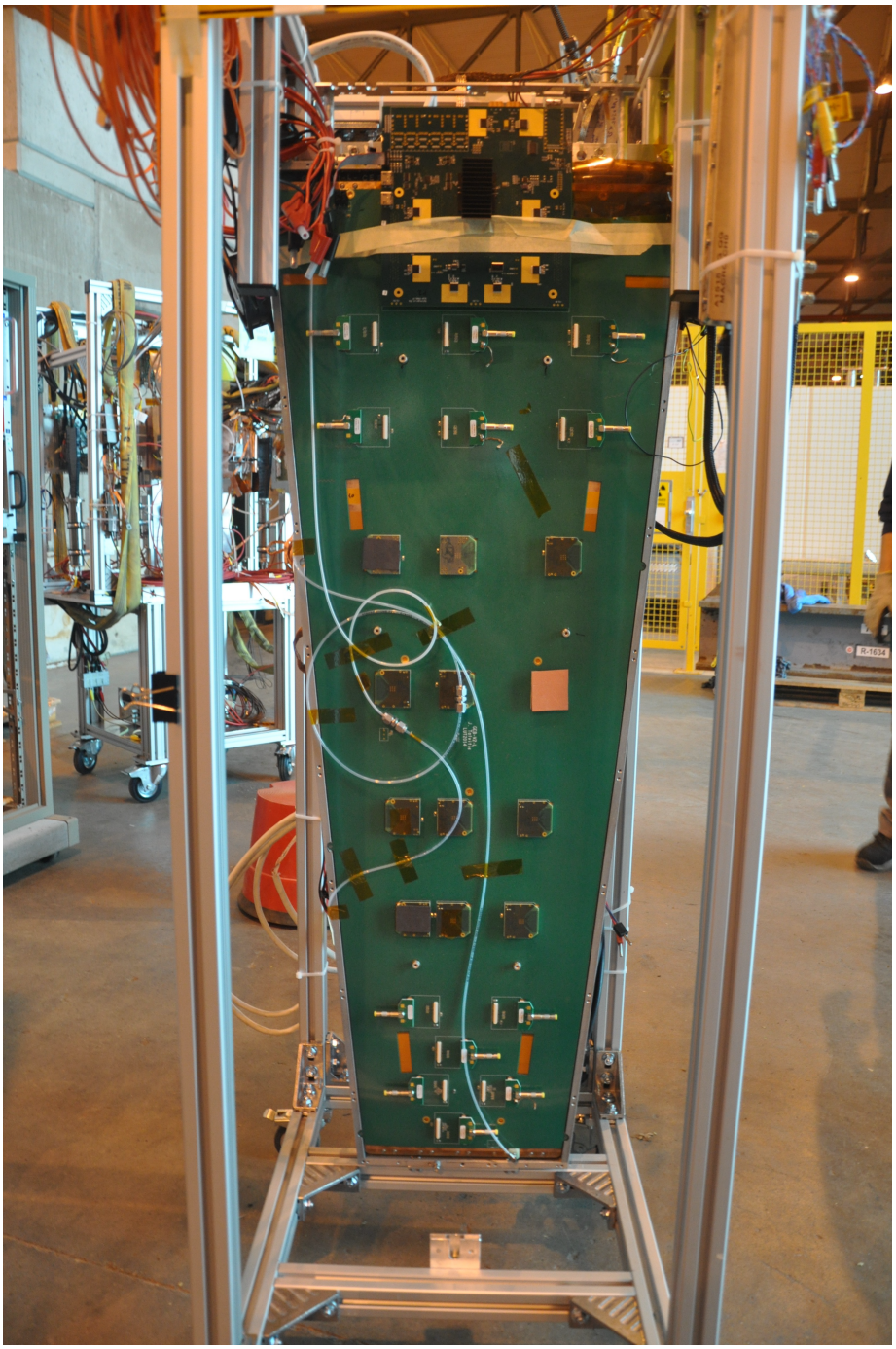

Figure 5.1: Fully-equipped GEM chambers used in the test beam [21]

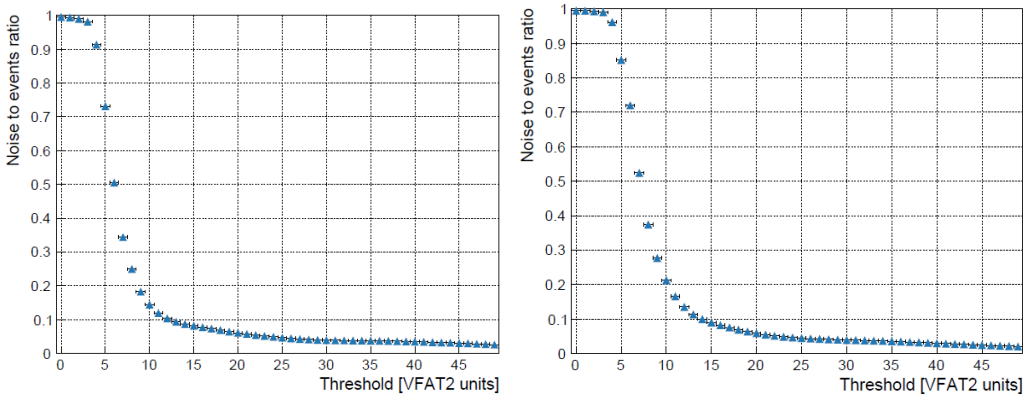

(a) Threshold Scan on GEM0 (b) Threshold Scan on GEM1

Figure 5.2: Threshold Scans performed during Test Beam [21]

WebDAQ is used to perform the scans, shown in Fig. 5.3. The latency is thus set to 11 to maximize the probability of retrieving the correct event upon receipt of a level-1 accept (L1A) trigger. Latency scans can also be used to measure the noise characteristic of the chambers, since all out-of-time events result from noise. This noise is still present for the in-time events, so it important to understand its magnitude relative to the signal.

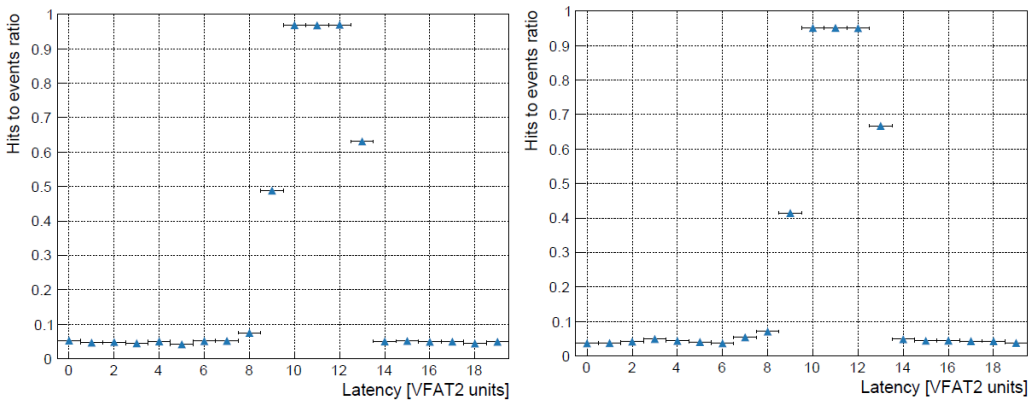

(a) Latency Scan on GEM0 (b) Latency Scan on GEM1

Figure 5.3: Latency Scans performed during Test Beam [21]

5.2.2 Noise Investigation

Two major sources of noise were identified following the noise investigation during the test beam campaign. One of the communication lines which provided slow-control of the VFAT2s via I2C protocol was found to introduce noise at 100 kHz, the same as the clock frequency for these lines. This problem was solved by activating the I2C clock during slow-control commands only, which reduced noise on the trigger bits. Additionally, it was discovered that current loops between the low-voltage cables powering the OptoHybrid and input trigger signal lines were introducing noise as well. The grounds for both of these were connected via shielding on the input trigger cables which solved this issue. Once these two problems were identified and solved, noise levels returned to expected values from previous runs.

5.2.3 Data Quality Monitoring

The Fall 2015 Test Beam was one of the first applications of the described DQM software of this thesis work on real data. The primary goals of the DQM were to ensure data integrity, monitor the beam profile and chamber occupancy, verify expected cluster size and multiplicity, and check for any firmware problems during data taking. Most of these were monitored via summary canvases outlined and detailed in Chapter 4.

One of the more insightful and interesting plots produced by the DQM for a test beam is the 2D Occupancy, or Beam Profile. When viewed in the Local DQM Browser, the occupancy canvas appears as shown in Fig. 5.4. This displays the canvas of only one of the chambers in the Test Beam, however. The beam profile for both chambers are overlayed and shown in Fig. 5.5. The beam is clearly shown for both chambers by the Gaussian curve in eta partition 4, which is also reflected in the 2D occupancy plots. The other eta partitions show spikes associated with noisy channels.

An important check performed by the DQM is on data integrity. The integrity canvas

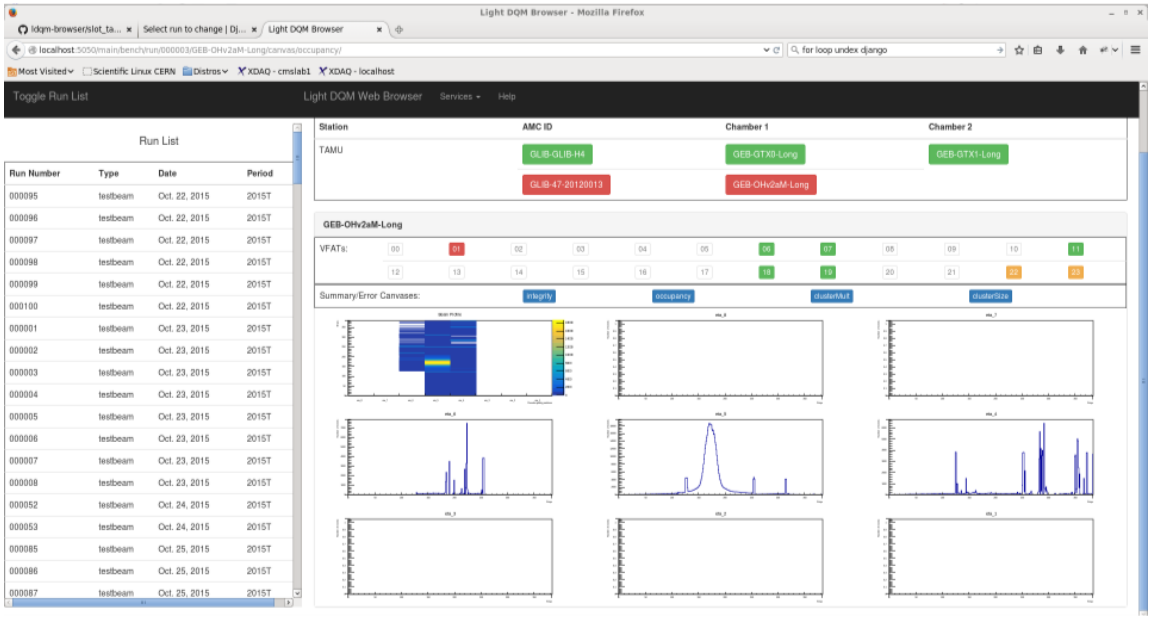

Figure 5.4: Test Beam Profile for single chamber as seen in DQM Browser: Top Left - 2D Occupancy; Following - 1D Occupancy by Eta Partition

identifies problems with data corruption at the VFAT level, and is shown in Fig. 5.6. The first three plots display the control bits, which, as expected, are constant meaning that no single-event upsets (SEU) occured on this part of the data. The bottom-left plot shows VFAT responses per event by slot number. This is expected, and shown, to be constant at 1 for present VFATs, because all VFATs are supposed to respond for every triggger. As mentioned before, not all VFAT slots were filled for the test beam. The plot to the right of this one is a similar check, plotting the number of VFATs responding per event. 8 VFATs were expected to respond, however only 7 are shown by these two plots. This indicates a problem with the VFAT in slot 19, which responds very seldomly. The final check is the cyclic redundancy check (CRC), which checks the entire data packet for SEU. It compares a received check sum with a recalculated (expected) one, and this comparison is plotted in the final two integrity plots.

Cluster Size and Multiplicity are the final summary canvases analyzed. They are shown

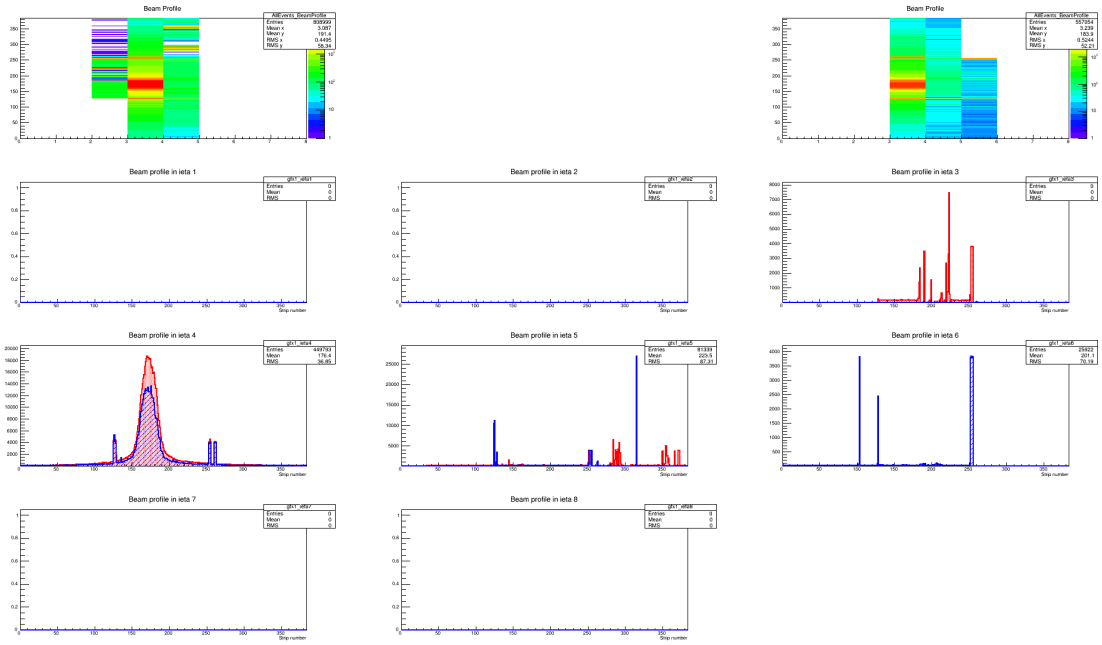

Figure 5.5: Test Beam Profile for both GEM chambers: Top Left - 2D Occupancy for GEM0; Top Right - 2D Occupancy for GEM1; Following - Combined 1D Occupancy by Eta Partition with GEM0 in Red and GEM1 in Blue

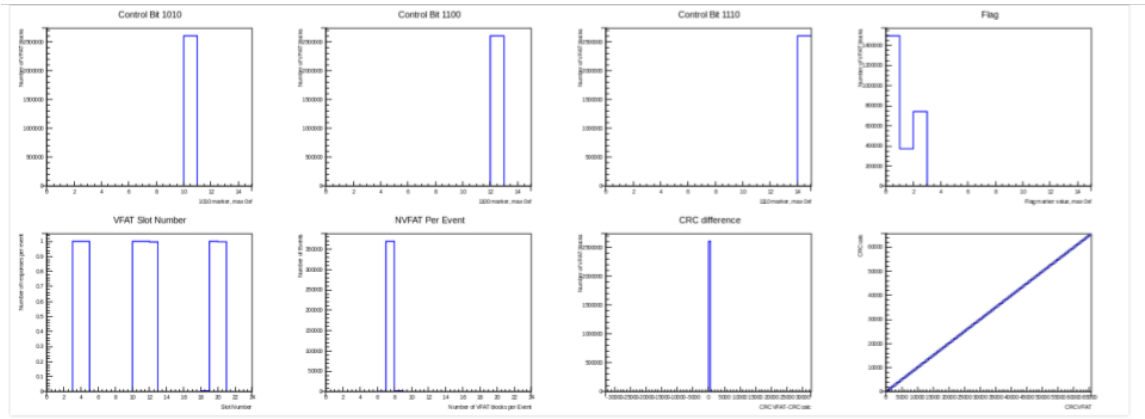

Figure 5.6: Test Beam Integrity Summary Canvas

in Fig. 5.8 and 5.7, respectively. Similar to the occupancy canvas, the plots are split into the full chamber in the top right and eta partitions between 1 and 8 following.

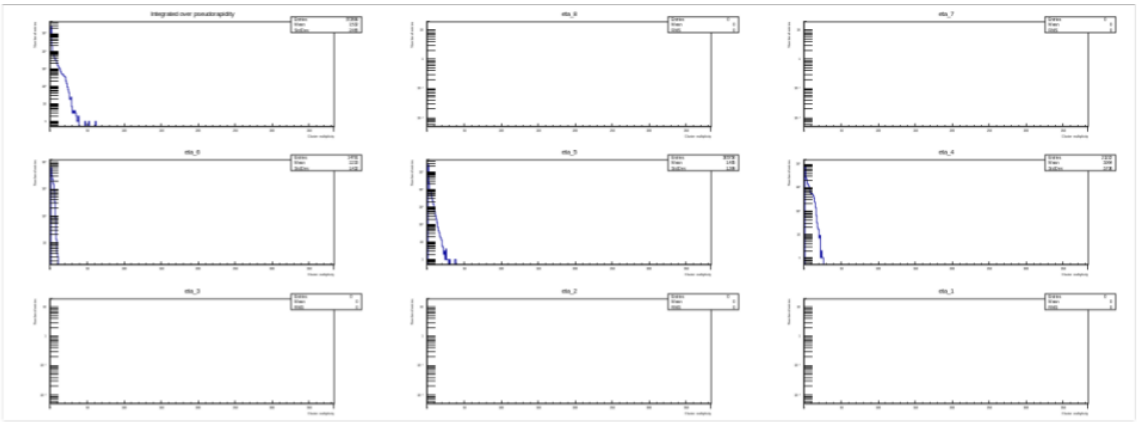

Figure 5.7: Test Beam Cluster Multiplicity Summary Canvas

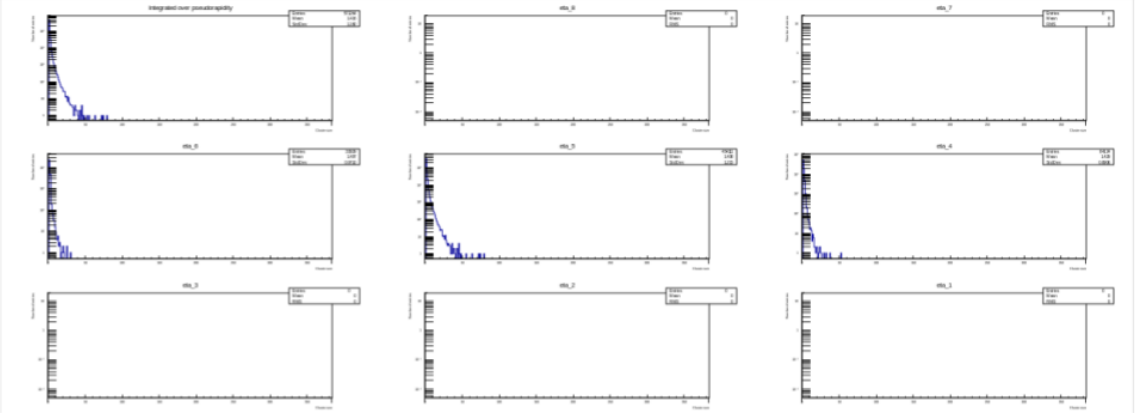

Figure 5.8: Test Beam Cluster Size Summary Canvas

In addition to the summary canvases, numerous hardware-specific histograms are also included in the DQM software. These are used to identify problems with specific electronics, and can help trace down the source of larger problems observed, for example, in the summary canvases.

5.3 Cosmic Stand at Tracker Integration Facility

The GEM integration test stand performs all quality control steps for the GEM chambers before they are transported to be placed underground in CMS. The first major mile-

stone for this facility is the production and verification of the 5 super-chambers to be installed in the Slice Test at the end of 2016. Leading up to this, a thorough set of quality control steps were defined to be performed on all GEM chambers.

One of the final steps in the quality control process is installation of chambers in a cosmic stand. The chambers are placed between scintillators horizontally in order to take cosmic muon measurements. The full setup is shown in Fig. 5.9. This allows analysis of cluster size, timing, and overall efficiency of the detectors. The coincidence of the scintillators provides the trigger logic for the GEM chambers when a cosmic muons passes through the full setup.

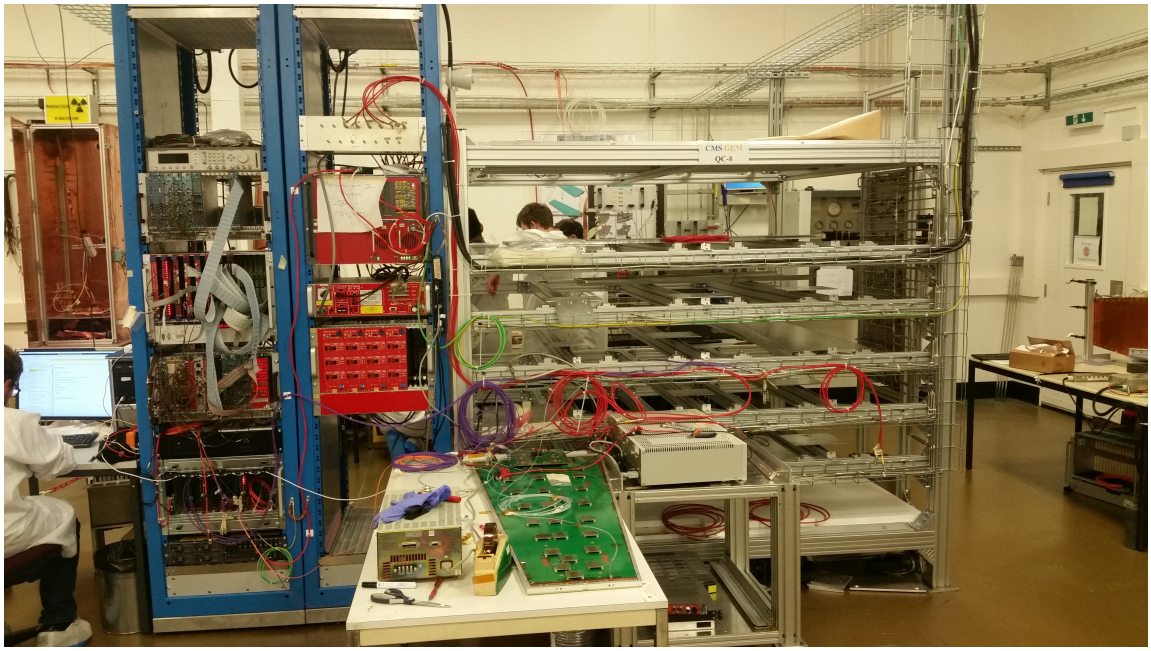

Figure 5.9: Initializing DAQ station at Cosmic Stand at the Tracker Integration Facility: left shows DAQ electronics station including μTCA crate (blue); right shows Cosmic Stand before chambers are installed in between the scintillators on top and bottom layers

5.3.1 Data Quality Monitoring

Similar to the Test Beam campaign, the Cosmic Stand also requires DQM software to validate the GEM cosmic data. Because data is being taken from cosmic muons, the trigger rate is significantly lower than during normal operation in CMS, so the electronics are expected to have no problem handling the data rate. Another result of taking data from cosmic muons is a uniform distribution. This uniformity is verified in the 2D occupancy plots for two chambers forming a super-chamber shown in Fig. 5.10 and 5.11. The distribution of hits across both chambers is relatively uniform, considering the limitations of plotting a trapezoidal area onto a rectangular plot.

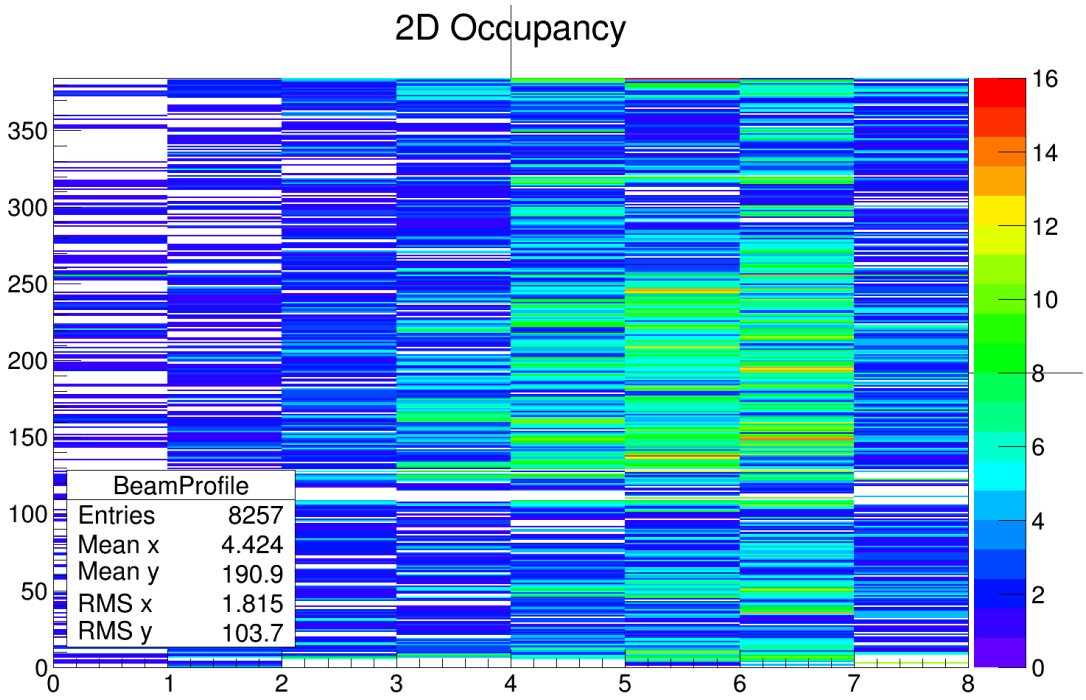

Figure 5.10: 2D Occupancy Plot for GEM0 of super-chamber in the Cosmic Stand

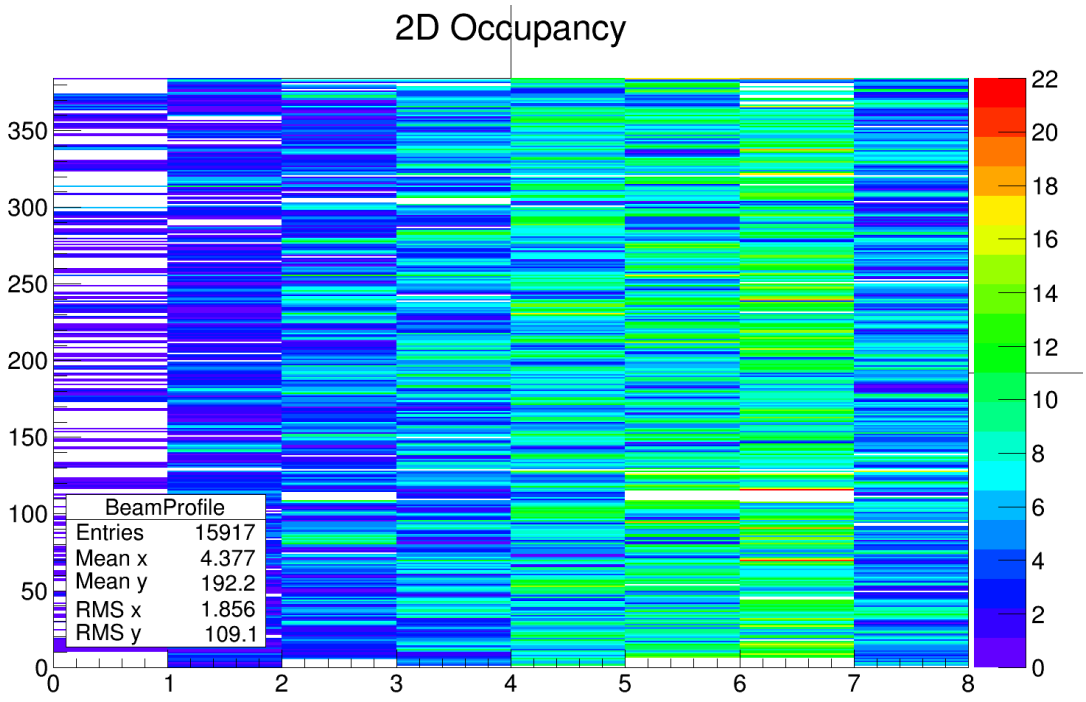

Figure 5.11: 2D Occupancy Plot for GEM1 of super-chamber in the Cosmic Stand

The DQM is also used to look into the data integrity and characteristics of the clusters received. Because there is not a large amount of SEU from cosmic particles, data integrity is expected to be good. Fig. 5.12 shows the control bit plots displaying perfect reception of control bits from all data packets. Similarly, no CRC errors were recorded for this data run. The cluster size distribution is shown in Fig. 5.13, and is around expected values. Average hits should only activate around 2 or 3 strips to form a cluster, in order to meet resolution requirements.

5.3.2 Addition of Radiation Source

One data run is taken on the cosmic stand with the addition of a radiation source. It is placed at four different positions in order to cross-check the strip to channel mapping at certain eta partitions. The radiation source provides a high flux of particles causing hits in

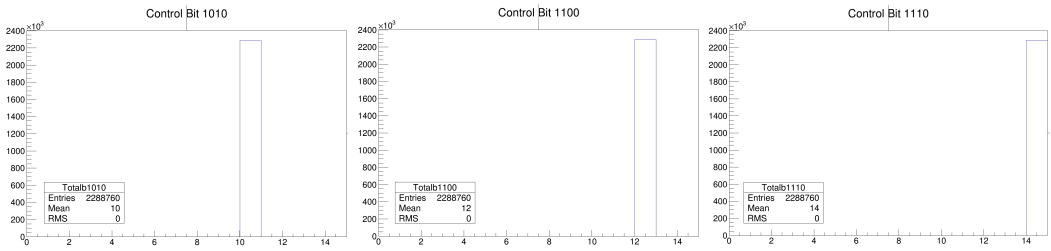

Figure 5.12: Control Bit plots for cosmic data run

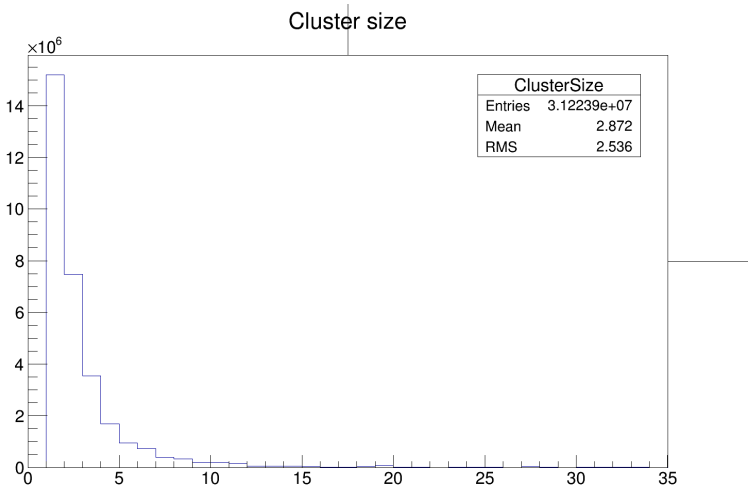

Figure 5.13: Cluster Size distribution for cosmic data run

the specific regions that it is placed near the chamber. DQM performed on this run shows the effects that the radiation source has on the resulting data.

The 2D occupancy plot, shown in Fig. 5.14, clearly shows the four locations where the source has been placed on the chamber. The peak heights depend on the amount of time the source is left in each specific location. Fig. 5.15 shows the eta partitions containing the two largest peaks, namely eta 6 and eta 7.

The radiation source not only causes a higher hit rate, but also causes more SEUs from radiation passing through the electronics. This data corruption is evident in the integrity

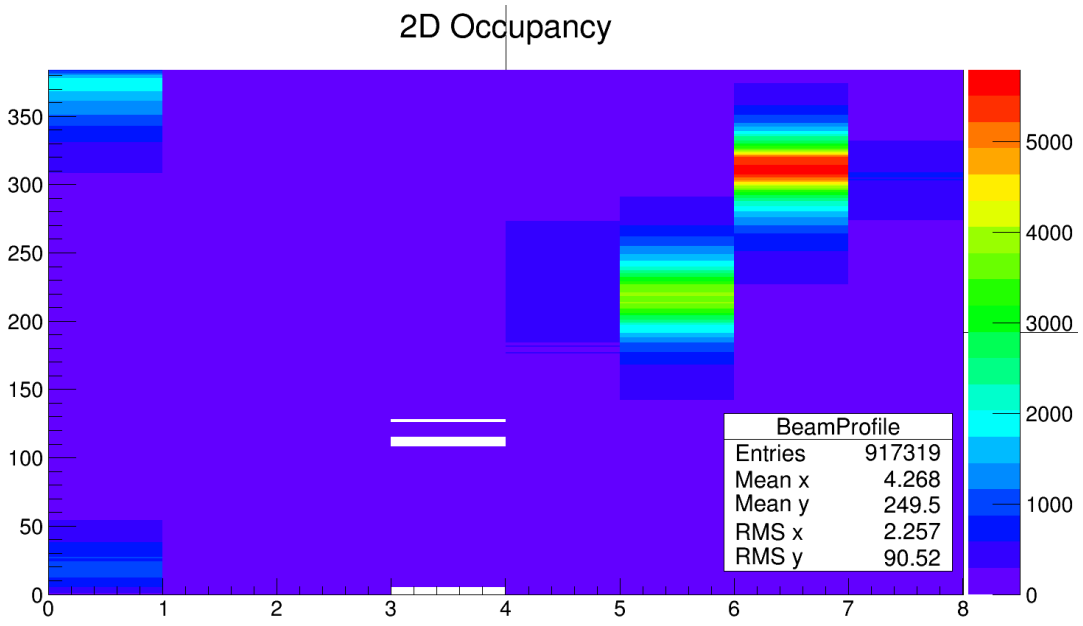

Figure 5.14: 2D Occupancy Plot for chamber under radiation source testing

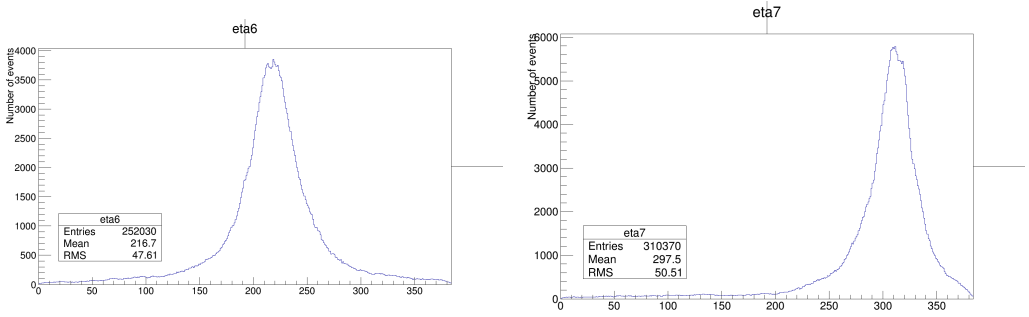

Figure 5.15: Eta Partitions from Beam Profile of chamber under radiation source testing

checks performed by the DQM. Fig. 5.16 shows the control bit plots for the data run with the radiation source, plotted on a log scale. There are occasional corrupted events throughout the data run, corresponding to the incorrect received control bits. This is expected in a highly irradiated environment, and there are methods in place to correct these errors.

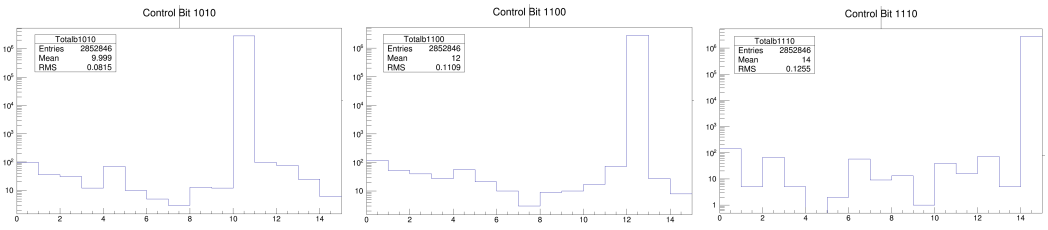

Figure 5.16: Control Bit plots for chamber under radiation source testing

5.4 Cathode Strip Chamber Integration at Building 904

One of the steps to integrating the GEM system with the rest of CMS is integrating GEMs with cathode-strip chambers (CSC). Trigger data from GEMs and CSCs is combined for an improved muon trigger system upon installation of the GE1/1 system. Therefore, it is imperative that these chambers are able to synchronize and combine their trigger data. An integration stand is set up in building 904 at CERN, which has up to two GEM chambers and one CSC chamber installed horizontally for cosmic muon measurement. The full GEM DAQ electronics system is installed on this test stand as well, providing an excellent location for software and firmware development for both systems.

This test stand provides the resources necessary to develop and run the CTP7 SBit scan. The GEM trigger data (SBits) are transmitted to both the CTP7 and the CSC optical trigger motherboard (OTMB). In order to combine the GEM trigger data with CSC data, it must be characterized and verified. Upon its installment, this test stand is the only location where real GEM trigger data can be combined with real CSC trigger data. Using the CTP7 SBit scan, the SBit encoding was verified and then transmitted successfully to the CSC OTMB. The firmware to translate and use this data in trigger logic has been developed with the help of this software.

5.5 Slice Test

The largest checkpoint before the full installation of GE1/1 in CMS is the Slice Test. Five super-chambers, nicknamed "GEMINI" for the "twin" GEM chambers, have been installed underground in CMS during the extended year-end technical stop of 2016. These chambers have now been fully commissioned and are currently undergoing routine calibration scans. The DQM software is not yet installed at Point 5, but is expected to soon.

5.5.1 Calibration Scans

As with any setup, when the chambers are initially installed they must be calibrated. After initial powering of the system, one of the first tests performed is the s-curve scan, in order to characterize the noise of the system and begin to set the proper threshold. S-curve scans are performed for each chamber, which are represented as in Fig. 5.17. Each plot represents a different VFAT2 on a single chamber, and each column represents a different strip. This essentially combines 128 individual 1D s-curve plots into a single plot. Color indicates the amount of hits as calibration pulse height is increased.

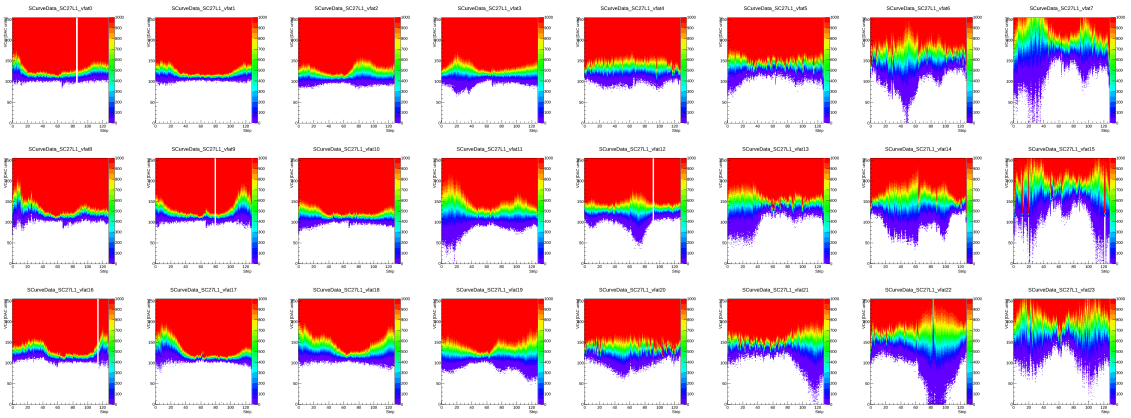

Figure 5.17: SCurve Results from chamber in Slice Test

As shown, some VFAT channels perform better than others. A scan is performed to mask, or turn off, noisy channels which do not respond as expected. The results from the same chamber after noisy channels have been masked is shown in Fig. 5.18.

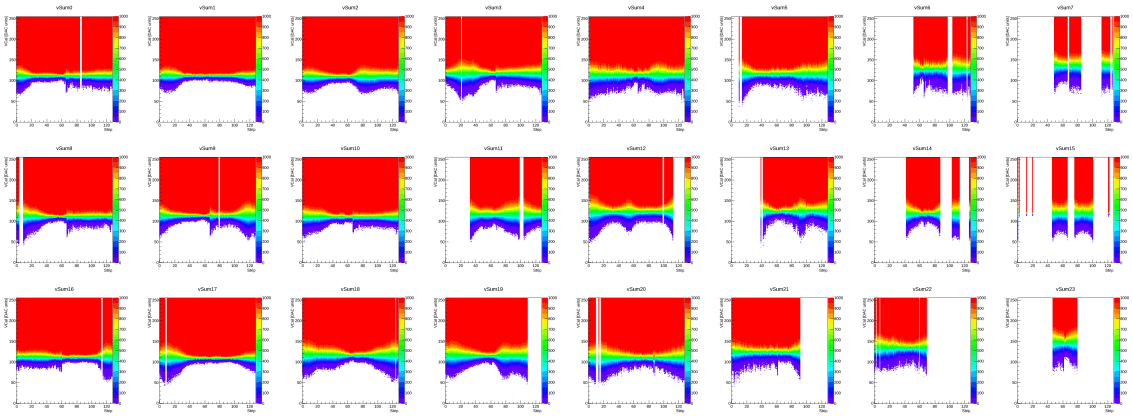

Figure 5.18: SCurve Results from chamber in Slice Test with masked channels

CHAPTER 6

SUMMARY AND CONCLUSIONS

The GEM DAQ electronics and software are still under development in preparation for the full GE1/1 station installation in 2019 and beyond. GEM chambers utilizing version 2 electronics have been installed in CMS at the end of 2016 in the GE1/1 Slice Test. The results of the Slice Test as well as ongoing research and development at test stands are contributing to the design and production of new version 3 electronics which will be used in the final installation. These developments and improvements will be outlined in this chapter, ending in a finalizing conclusion.

6.1 Ongoing Developments

One of the major ongoing developments is transitioning from version 2 to version 3 electronics. This includes a major redesign of the on-detector electronics. The GEB will be split into two separate boards with a new version 3 OptoHybrid placed in between and connecting the two. The goal is to eliminate noise and decreased signal quality associated with the long high-speed signal lines of the current GEB design. The smaller design will also eliminate the manufacturing challenges of fabricating the nearly meter-long version 2 GEB.

Table 6.1: Evolution of DAQ system for GE1/1 [21]

	First Prototype	**Test Beam**	**Slice Test**	**Final System**
Front-End	6x VFAT2	24x VFAT2	24x VFAT2	24x VFAT3
GEB	GEB v1	GEB v2	GEB v2	GEB v3
OptoHybrid	OH v1	OH v2a	OH v2b	OH v3
AMC	GLIB	GLIB	CTP7	CTP7

The VFAT3 is also under development by a team at CERN to improve the currently-employed VFAT2. The new front-end chips will use the GigaBit Transceiver (GBT) chipset, rather than being controlled and readout by the FPGA on the OptoHybrid. The trigger granularity will be increased from 8 bits per BX to 64 bits per BX, allowing for a total resolution of 2 strips in the trigger data. The VFAT3 will also feature programmable gain and shaping time, larger memory depth, and improve data packet structure and slow control functionality [11].

The Light DQM software has been designed with the ongoing changes and transition from version 2 to version 3 electronics in mind. The software is flexible and will require little to no adjustment with the advent of the new hardware.

6.1.1 CTP7 Development

Due to the price and necessity of the CTP7 board, there are very few locations with access to a free (not data-taking) CTP7 board. Of these locations include building 904 at CERN and Texas A&M. Thus, most CTP7 developments are performed at these two locations. Current developments include monitoring applications, implementation of remote procedure calls (RPC), and firmware development.

One of the major advantages of the CTP7 is its on-board ZYNQ SoC, more specifically the timing improvements it offers with regard to monitoring and scan applications. Reading or writing registers on the CTP7 FPGA from a DAQ PC via current standard protocols takes on the order of 100 ms per register. The ZYNQ SoC, however, can perform the same operation between 4 and 10 μs. To fully take advantage of this architecture, implementation of remote procedure calls (RPC) is currently under development for register-intensive procedures. RPCs are a relatively standard protocol in which one program or computer calls upon another to perform a routine. For the CTP7, such calls are sent from a DAQ PC via TCP/IP protocol to the CTP7 ZYNQ SoC to initiate register-intensive routines which

it can perform much faster.

One of the primary use-cases of RPCs is reprogramming connected OptoHybrid firmware from the CTP7. When the electronics are installed underground, they will be inaccessible and will need a valid way to reprogram the firmware if necessary. This can be done via the CTP7 by writing to nearly 1.6 million registers. Such a task is easily implementable as an RPC. Initial testing has shown that this can be done in around 30 seconds using RPCs, whereas it would have taken tens of hours writing registers from the DAQ PC directly.

The CTP7 firmware, which defines the behavior of the on-board FPGA, has been adopted and developed from firmware written for the previous AMC, the GLIB. This new firmware has been developed to be board-agnostic, meaning it can be compiled to work on any AMC architecture with a compatible FPGA. This makes development and version control much simpler, because the new firmware, and any future updates, are able to run on both CTP7 and GLIB. This new style of AMC firmware has been appropriately named "common" AMC firmware. To summarize, common AMC firmware can be used at any test stand regardless of its AMC hardware, allowing for more synchronous development.

6.2 Planned Improvements and Applications

One of the short-comings of the GEM DQM software is that is has not been integrated with scan routines very effectively. Initial versions of the browser included the possibility to view the results of threshold scans only. This feature was not utilized because these scans were instead included with the WebDAQ application, which would both perform and display the scans. Because these scans, as well as others, are normally only needed to quickly initialize the system, rather than used in offline analysis, the WebDAQ was a more natural fit for them. As shown in the results from the Test Beam, certain scans are used in offline analysis as well as initialization of the system. In this regard, full integration of scan routine results with the rest of the DQM browser could help with such analysis in the

future.

Certain scans, such as those used in quality control of VFATs and s-curve scans, are currently performed using Python scripts which produce data files that are manually manipulated and viewed. The DQM browser, or a similar adaptation, is a perfect tool to view the results of such scans for improved organization and result comparison between hardware and different configurations. In addition, the DQM daemon which oversees the DQM analysis is written in Python, making integration with Python scripts very straightforward. A slight overhead of integration or adaptation of current code would be necessary, but this could dramatically improve such processes.

6.3 Conclusion

As part of the CMS muon system upgrade taking place in 2019, novel GEM detectors are under development for implementation in the high-eta region of CMS. Customized data-acquisition electronics are being developed in parallel. Thorough testing and monitoring applications are required to calibrate the detector electronics and validate the data that they produce.

We have developed data quality monitoring software as the principle part of this thesis work which implements automated analysis and simple browsing of current and past data runs. The software can be used to monitor elements of active runs or compare past runs with full-granularity for more in-depth offline analysis. It is expandable to function with any amount of hardware, and stores configurations in a central database. Furthermore, any type of data analysis desired can be easily added to the software to be applied to all data runs.

This data quality monitoring software has been deployed to various GEM test stands around the world. Most recently, it is in the process of being installed at P5 to monitor the GEM chambers which have been installed in CMS for the Slice Test. We look forward to

using this software on data taken by these detectors in the near future. The data received and analyzed from the Slice Test will help further develop this software in order to perfect it for implementation with the full GE1/1 system in 2019, when the amount of chambers and data size will require a robust software system for effective analysis.

REFERENCES

[1] A. Colaleo, A. Safonov, A. Sharma, and M. Tytgat, "CMS Technical Design Report for the Muon Endcap GEM Upgrade," Tech. Rep. CERN-LHCC-2015-012. CMS-TDR-013, Jun 2015.

[2] C. Lefevre, "LHC: the guide (English version). Guide du LHC (version anglaise)," tech. rep., Feb 2009.

[3] The CMS Collaboration, "The CMS experiment at CERN LHC," *Journal of Instrumentation*, vol. 3, no. 08, p. S08004, 2008.

[4] S. Chatrchyan and K. et all., "Measurement of the properties of a higgs boson in the four-lepton final state," *Phys. Rev. D*, vol. 89, p. 092007, May 2014.

[5] A. Tapper and D. Acosta, "CMS Technical Design Report for the Level-1 Trigger Upgrade," Tech. Rep. CERN-LHCC-2013-011. CMS-TDR-12, Jun 2013.

[6] P. Moreira, R. Ballabriga, S. Baron, S. Bonacini, O. Cobanoglu, F. Faccio, T. Fedorov, R. Francisco, P. Gui, P. Hartin, K. Kloukinas, X. Llopart, A. Marchioro, C. Paillard, N. Pinilla, K. Wyllie, and B. Yu, "The GBT Project," 2009.

[7] F Vasey et all, "The versatile link, a common project for super-LHC," *Journal of Instrumentation*, vol. 4, no. 12, p. P12003, 2009.

[8] M. Lazzaroni, "Power distribution for the ATLAS LAr Trigger Digitizer Board," *Journal of Instrumentation*, vol. 11, no. 01, p. C01042, 2016.

[9] T. T. C. et all, "The totem experiment at the cern large hadron collider," *Journal of Instrumentation*, vol. 3, no. 08, p. S08007, 2008.

[10] P. Aspell, G. Anelli, P. Chalmet, J. Kaplon, K. Kloukinas, H. Mugnier, and W. Snoeys, "VFAT2: A front-end system on chip providing fast trigger information, digitized data storage and formatting for the charge sensitive readout of multichannel silicon and gas particle detectors," p. 5 p, 2007.

[11] M. Dabrowski and P. Aspell et all, "The VFAT3-Comm-Port: a complete communication port for front-end ASICs intended for use within the high luminosity radiation environments of the LHC," *Journal of Instrumentation*, vol. 10, no. 03, p. C03019, 2015.

[12] VadaTech, "Vadatech vt892."

[13] E. Hazen, A. Heister, C. Hill, J. Rohlf, S. X. Wu, and D. Zou, "The amc13xg: a new generation clock/timing/daq module for cms microtca," *Journal of Instrumentation*, vol. 8, no. 12, p. C12036, 2013.

[14] "The cms xdaq project," Dec 2016. https://svnweb.cern.ch/trac/cmsos.

[15] L. Borrello, "The Data Quality Monitoring Software for the CMS experiment at the LHC," Tech. Rep. CMS-CR-2014-431, CERN, Geneva, Nov 2014.

[16] U. Guide, "Root a data analysis framework," May 2014. https://root.cern.ch/root/htmldoc/guides/users-guide/ROOTUsersGuide.html.

[17] CERN, "Proof | root a data analysis framework."

[18] "The django project." https://www.djangoproject.com/.

[19] "Python documentation: cmd - support for line-oriented command interpreters." https://docs.python.org/2/library/cmd.html.

[20] D. A. et all, "Quality control and beam test of gem detectors for future upgrades of the cms muon high rate region at the lhc," *Journal of Instrumentation*, vol. 10, no. 03, p. C03039, 2015.

[21] T. Lenzi and G. De Lentdecker, "Development of the DAQ System of Triple-GEM Detectors for the CMS Muon Spectrometer Upgrade at LHC," tech. rep., 2016. Presented 19 Dec 2016.

ABBREVIATIONS

AMC Advanced Mezzanine Card

BX Bunch Crossing

CCB Clock and Control Board

CSC Cathode Strip Chamber

CMS Compact Muon Solenoid

CRC Cyclic Redundancy Check

CTP7 CTP7 board

DAQ Data Acquisition

DQM Data Quality Monitoring

FPGA Field-Programmable Gate Array

GBT(x) Gigabit Transceiver

GEB GEM Electronics Board

GEM Gas Electron Multiplier

GLIB Gigabit Link Interface Board

L1A Level-1 Accept

LHC Large Hadron Collider

MTF Muon TrackFinder

OH OptoHybrid

OTMB Optical Trigger MotherBoard

P5 Point 5

SEU Single-Event Upset

SoC System-on-Chip

TTC Trigger Timing and Control